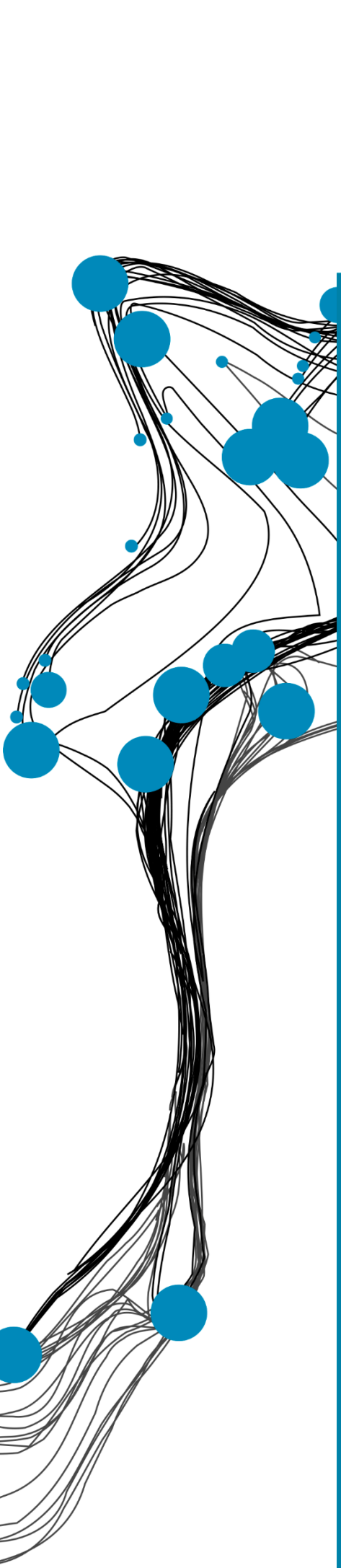

Thesis – Master Biomedical Engineering 30th of January 2024

Correlation between chronic complaints in mild traumatic brain injury patients and quantitative electroencephalography

Timon van Zijp

Faculty of Science and Technology
Clinical Neurophysiology

Supervisors:
V. Barone - PhD
M.E. de Koning - MD, PhD
M.C. Tjepkema - Cloostermans - PhD

Chair assignment committee:
M.J.A.M. van Putten - Prof., MD, PhD

External member assignment committee:
T. Heida - Prof., PhD

UNIVERSITY OF TWENTE.

Acknowledgments

Many directly and indirectly contributed to my graduation research and I am grateful for all the time and effort they spend to make my research possible. First of all, I like to thank my daily supervisors, Valentina Barone, Marleen Tjepkema and Myrthe de Koning for their expertise, insights and very valuable feedback. I would like to thank Ciska Heida for her role as external member of the assignment committee and likewise I would like to thank Michel van Putten for his role of chair of the same committee. I would also like to thank Job van der Palen on his advice on statistics.

I want to thank all patients who, often in painful and awkward circumstances right after an accident, showed willingness to participate. I like to thank the mTBI patients that shared their, sometimes painful yet inspiring, stories. The inclusion of patients and the recording of EEG-data was realised by neurologists, technicians and staff members at the Department of Neurology at the Medisch Spectrum Twente in Enschede, as well as by Valentina Barone; I am grateful for their effort.

I would like to thank my parents and sister; they have shown valuable support (and patience). I like to thank Liesbeth van Zijp for providing a valuable spelling check on my entire thesis. I am grateful for the support that I received from many students and PhD candidates (many related to the Clinical Neurophysiology group and many related to my student association). I am grateful for the wisdom and advise from the BME study advisors and the participants of the BME graduation group.

I am grateful for all supervisors that were involved in my previous graduation research attempt. Despite the fact that the previous attempt was eventually cancelled, it turned out to be an instructive process, made possible thanks to the effort of many.

Many have shown support, patience, empathy and benevolence, for which I am all very grateful. My thanks is to all of you!

"… test them all; hold on to what is good,…" - 1 Thessalonians 5: 21 (NIV)

Abstract

Background

Mild traumatic brain injury (mTBI) is a very common condition, having an estimated incidence of over 600 per 100,000 per year. Although most mTBI patients recover well within weeks to months, 15 – 30% suffer complaints long after trauma, interfering with outcome. Currently, no reliable method exists to, in an early stage, predict which mTBI patients are at risk of developing persistent complaints. In this explorative study, we searched for possible correlations between EEG characteristics and outcome after mTBI.

Methods

We used EEG-data from 23 acute (<24 hours after trauma) and 26 subacute (4 – 6 weeks after trauma) mTBI patients (23 overlap). After 6 months, the persistence of complaints was assessed with the Head Injury Symptom Checklist (HISC) and recovery was assessed with the Glasgow Outcome Scale – Extended (GOS-E) questionnaire. We performed signal analyses on the EEG-data using four different techniques: relative power, power variability, power symmetry and coherence. To correct for heterogeneity (of the trauma) of the patients and to limit the number of statistical comparisons, we only statistically analysed data from the leads or lead-pairs that, per patient, diverge most from healthy reference values. We used the Spearman's rank correlation coefficient test and the Mann-Whitney U-test to compare the results of the signal analyses to the HISC scores and to the GOS-E outcomes respectively.

Results

We found three possible correlations. First, patients with fewer or no persistent complaints have lower relative alpha power in the acute phase compared to the subacute phase (correlation value = -0.44, P = 0.04). Second, subacute patients with more persistent complaints have lower theta power variability than healthy average (correlation value = -0.43, P = 0.03). Third, acute phase patients have a lower coherence than healthy average and those with a poor recovery have an even lower coherence than those with good recovery (P = 0.04).

Conclusion

In our study we found three possible correlations between EEG characteristics and outcome after mTBI. We recommend to focus future research on validating our findings in large cohorts. Alternatively, future research could also be focused on implementing our findings in a machine learning system.

Samenvatting

Achtergrond

Licht traumatisch schedelhersenletsel (LTSH) is een veelvoorkomende aandoening; de incidentie wordt geschat op meer dan 600 per 100.000 per jaar. Alhoewel de meeste LTSH patiënten binnen weken tot maanden herstellen, behoudt 15 – 30% van de patiënten lang na trauma klachten. Momenteel bestaat er geen methode om vroegtijdig te voorspellen of een LTSH patiënt risico loopt op het ontwikkelen van aanhoudende klachten. In dit exploratieve onderzoek hebben we gezocht naar mogelijke correlaties tussen EEG karakteristieken en herstel na LTSH.

Methode

We gebruikten EEG-data van 23 acute (<24 uur na trauma) en 26 subacute (4 – 6 weken na trauma) LTSH patiënten (23 overlap). Na 6 maanden hebben we de aanhoudendheid van klachten in beeld gebracht m.b.v. de Head Injury Symptom Checklist (HISC) en hebben we herstel beoordeeld m.b.v. de Glasgow Outcome Scale – Extended (GOS-E) vragenlijst. We hebben vier technieken gebruikt om signaalanalyses op EEG-data uit te voeren: relatief vermogen, vermogen variabiliteit, vermogen symmetrie en coherentie. Om te corrigeren voor de heterogeniteit (van het trauma) van de patiënten en om de hoeveelheid statistische vergelijkingen te beperken hebben we alleen statistische analyses uitgevoerd op data van kanalen of kanaalcombinaties die, per patiënt, het meest afwijken van gezonde referentiewaarden. We hebben de Spearmans rangcorrelatiecoëfficiënt test en de mann-whitneytoets gebruikt om de resultaten van de signaalanalyses met respectievelijk de HISC scores en de GOS-E uitkomsten te vergelijken.

Resultaten

We hebben drie mogelijke correlaties gevonden. Ten eerste, patiënten met weinig of zonder aanhoudende klachten hebben minder relatief alfa vermogen in de acute fase vergeleken met de subacute fase (correlatiewaarde = -0,44, P = 0,04). Ten tweede, subacute patiënten met meer aanhoudende klachten hebben minder thèta vermogen variabiliteit dan gezonde mensen (correlatiewaarde = -0,43, P = 0,03). Ten derde, patiënten in de acute fase hebben een lagere coherentie dan gezonde mensen en diegenen met slecht herstel hebben een lagere coherentie dan diegenen met goed herstel (P = 0,04).

Conclusie

In ons onderzoek hebben we drie mogelijke correlaties gevonden tussen EEG karakteristieken en herstel na LTSH. We adviseren om toekomstig onderzoek te richten op het valideren van onze bevindingen. Als alternatief zou toekomstig onderzoek ook gericht kunnen worden op het implementeren van onze bevindingen in een machine learning systeem.

Contents

Background

Mild traumatic brain injury (mTBI) can be defined as *"… acute neurophysiologic brain dysfunction resulting from impact contact forces or sudden acceleration/deceleration causing a transient alteration of consciousness and/or a period of anterograde (and possibly retrograde) amnesia."* [1]. It is a common condition; the estimated incidence is over 600 per 100,000 [2]. Most mTBI victims recover well within weeks to months, although an estimated 15 – 30% experience symptoms long after trauma [3]. Currently, no proper method exists to predict which patients are at risk of suffering long-term complaints. This master graduation research focusses on predicting the risk for poor outcome using EEG.

1. Definitions

The severity of traumatic brain injury is defined by the Glascow Coma Scale (GCS), a scale ranging from 3 – 15, measuring the depth of a coma directly after trauma [4,5]. TBI patients with a GCS score of 13 – 15 are usually considered mild. Such a GCS range suggests that the patient is with conscious, though their consciousness can be slightly altered (for example, the patient can have a confused or inappropriate verbal response). Besides this GSC range, for a TBI patient to be considered of the mild category, a patients must have either a loss of consciousness not exceeding 30 minutes or a period of post-traumatic amnesia must not exceeding 24 hours [6].

2. Incidence and causes

Most (70 – 90%) hospital treated TBIs are a mild TBI [2]. The global mTBI incidence is estimated at 100 – 300 per 100,000 [2]. However, the true population based incidence, including mTBI victims not treated in hospitals (for instance when only visiting a primary care physician), may very well exceed 600 per 100,000 [2].

In the Netherlands the incidence of all TBIs (including mild) is 213.6 per 100,000, based on data of TBI patients admitted to Dutch emergency departments [7]. Most TBIs are caused at home or while practicing leisure (47.9%), often due to falls. Traffic is also a major contributor to TBIs (33.5%) of which bicyclists seem to suffer most often (56.9% of traffic related TBI). Sport comes third as TBI contributor (8.1%). Assaults represented an estimated 6.5% of all Dutch TBIs. TBIs are most common in children, young adults and elderly. The incidence in males (241.9) is higher than in females (175.3) [7].

3. mTBI related forms of brain damage

Several mechanisms may be involved in traumatic brain damage (not specifically considering mTBI). Most obvious is the neural and axonal damage caused by the direct impact itself. Another almost instant mechanism is the so called 'diffuse axonal injury', which is damage (partly) caused by rotational and shearing stresses due to deceleration of the brain [8]. Diffuse axonal injury sometimes also happens at the site opposite to the impact, due to the brain 'bouncing back' within the skull, which is known as the 'countrecoup effect' [9]. It is assumed that in practice, mTBIs are most often caused by frontal impact (due to people falling over in a forward manner). Therefore, the most frequent site of mTBI would be the frontal lobe of the cortex, although the occipital lobe is therefore also likely to be often damaged due to the countrecoup effect.

4. Prognosis

Most patients suffering mTBI recover well. Many though, suffer at least one symptom long after acquiring trauma. Estimates about this group range from 15 to 30% of all mTBI patients, which, calculated as an estimated incidence, would be 90 to 180 per 100,000, although it is not unlikely that the real incidence is even higher [2,3]. Many symptoms can be associated with chronic sequelae, including cognitive deficits (such as memory problems and attention difficulties), social inference (interpreting non-verbal and verbal social cues), psychological symptoms (anxiety, depression) and many physical problems (like fatigue, coordination problems and headache) [3].

mTBI is often associated with a reduced return to work (RTW) or school. Some studies report a return to work rate of 76% at 6 months and 5% to be on wage replacement benefits after 2 years [10]. These results are not unanimous and controversial findings have been reported. Cancelliere et al. report several factors (possibly) influencing an improved RTW including trauma related factors (such as absence of CT abnormalities), personal factors (such as 11+ years of formal education), and profession related factors in which professions having a more independent and decision-making latitude had a better RTW [10]. Although RTW and posttraumatic complaints are likely to be related, a one-to-one correlation cannot be assumed. Some predictors for poorer long-term mTBI recovery are older age, history of psychiatric conditions and lower educational level. It is speculated that individuals with mental health conditions prior to acquiring mTBI may have less reserve to deal with the additional burden of mTBI and individuals with a higher educational level may have developed better adaptive coping skills [11–13].

Besides the individual differences in presence and severity of posttraumatic complaints, the kind of complaints also differ. Gender may be a factor in these differences following mTBI [14]. High school females report complaints like drowsiness and noise sensitivity, while males more often had complaints like cognitive deficits and amnesia [14]. Females also tend to have more severe symptoms than males three months after trauma, possibly due to hormonal differences [15].

5. Prediction of posttraumatic complaints

When attempting to predict recovery in mTBI patients, conventional computed tomography (CT) as well as conventional magnetic resonance imaging (MRI) seem to be insufficient [16,17]. In the Netherlands, assessing a TBI patient via CT is common [18]. mTBI patients do however not very often show abnormalities on CT; in those with a GCS of 15 only 5% portray abnormalities and this percentage is 20 for those with a GCS of 14 and 30 for those of a GCS of 13 [17]. CT and MRI are unable to detect abnormalities of microstructural and functional nature. These conventional imaging techniques are therefore unable to detect abnormalities that may correlate to long lasting complaints, such as changes in the integrity of white matter pathways, abnormal brain activity, focal hypoperfusion and metabolism [16,19,20]. Although CT and MRI do not succeed in making such predictions, several other techniques may be interesting candidates, such as diffusion tensor imaging, single photon emission CT, magnetoencephalography and functional MRI. However, these candidates have shown mixed results or are unapplicable in clinical practice [1,19–21].

Biochemical biomarkers have also been researched, like S100B, neuron-specific enolase, glial fibrillary acidic protein, tau and neurofilament light, which in TBI patients are linked to poor long-term outcome. MicroRNAs are also speculated to be a possible biomarker for risk of poor outcome [22–29].

Quantitative electroencephalography (qEEG) research has been done in mTBI patients [30], though no articles are found specifically addressing the qEEG outcome differences between mTBI patients suffering persistent complaints and those not suffering these complaints. Despite this particular setting not being researched, the setting in the research of Tewarie et al. [31] was quite similar, albeit in moderate and severe TBI patients (GCS ≤ 12). They combined several (EEG) features into one model designed to predict outcome. Some of the features that played a prominent role were the Brain Symmetry Index (as designed by Van

Putten et al. [32]), variability in the alpha band, relative power in the alpha band, absolute power in the beta band and coherence. In total sixteen features were used, which also included non-EEG features like age, glucose and haemoglobin levels. According to Tewarie et al. the model had a fair to good specificity and sensitivity [31]. Other research was often not based on a model, but focused on one or a few EEG features. Vespa et al. measured the percentage of alpha variability (change of alpha wave activity) in severe and moderate TBI patients (GCS ≤ 14) in a continuous monitoring setting. They concluded that percentage of alpha variability is a sensitive and specific method of prognosis that is able to indicate outcomes in these patients [33]. In a review paper, Arciniegas [30] stated that in about 10% of mTBI patients EEG abnormalities such as low posterior alpha waves and mild diffuse intermixed slowing will remain in the late post-trauma period [30]. A research by Korn et al. [34] concluded that, when comparing TBI patients with persistent complaints to healthy individuals, the patients had higher delta (in this case defined as 1.5 – 5 Hz) power and lower alpha (8.5 – 12 Hz) power [34]. Other EEG-abnormalities that are often reported in mTBI patients are reduced mean alpha frequency, increased theta activity, increased theta-alpha ratio, increase in theta power variability, smaller difference in alpha and beta power when comparing anterior and posterior cortical regions, reduced posterior alpha power and an increase in coherence and decrease in phase between frontal and temporal cortical regions [30,35–40]. EEG-abnormalities in the first 24 hours post-trauma, in combination with other indicators may contribute to the prediction of poor long-term outcomes in TBI patients [30,31,41]. However, reports are inconclusive; some even report no EEG-abnormalities in TBI patients, even those with posttraumatic symptoms [30,42–46]. But even when EEG-abnormalities are found, causality may be questioned. Some of these abnormalities may be due to the effects of fatigue, anxiety and/or medication, according to Nuwer et al. [47].

6. Goal of study

Considering the high incidence of mTBI, the large percentage of mTBI patients suffering chronic complaints and the lack of a reliable outcome prediction tool, development of such a tool is of high importance. Regardless of attempts to predict the persistence of complaints in mTBI patients by means of conventional neuroimaging techniques such as CT and MRI, no conclusive method has been found. Biochemical biomarkers may be promising, though need more research (specifically into mild TBI). Some qEEG research has been done, though not specifically addressing the differences between mTBI patients with and without persistent complaints.

To develop such a tool, based on EEG, knowledge about the correlations between EEG characteristics and outcome is important. Therefore, the goal of this study is to search for potential correlations between EEG characteristics and the persistence of mTBI related complaints or the lack of recovery from mTBI. This study is of explorative nature, i.e. in this study we search for correlation candidates, rather than to prove correlations. Potential correlations found may (after validation in future research) contribute to the development of the needed prediction tool.

Methods

1. Participants

1.1 Patients group

We included thirty-one adult mTBI patients, admitted to the Medisch Spectrum Twente hospital in Enschede, the Netherlands. Electrophysiological (EEG) measurements were performed on the patients within the first 24 hours after injury (acute phase) as well as four to six weeks after trauma (subacute phase). Six months after trauma, the patients received questionnaires (which are explained later on in this chapter). We used these questionnaires to get information from the patients about persisting symptoms and recovery. Four patients did not return the questionnaires; they were excluded for further research. After correcting for missing and poor quality EEG-data, we included 23 patients with acute phase recordings and 26 patients with subacute phase recordings (23 overlap).

The inclusion criteria for the patient group were:

- The patient acquired a mTBI, in accordance with:
    - a Glasgow Coma Scale score of 13 – 15 during admittance at the emergency department with either
    - loss of consciousness, but not exceeding 30 minutes, and/or
    - post-traumatic amnesia, not exceeding 24 hours.
- The patient must be 18 – 80 years of age.

The exclusion criteria were:

- Neurological or psychiatric co-morbidity.
- Previous suffered TBI requiring hospital admission.
- Drugs or alcohol abuse.
- History of epilepsy.
- Cognitive impairment, language barrier or illiteracy compromising understanding and therefore completing of questionnaires.

1.2 Healthy control group

We included data from a healthy control population of 120 subjects from the Medical Spectrum Twente hospital for comparison. All subjects are considered healthy at the time of recording. Similar to the patient group, the control group subjects had to be at least 18 and at most 80 years of age. We matched average age of the control population (46.5 years) to the average age of the patient group (47.9 years).

2. Software

To visually inspect EEG-data and its annotations we used NeuroCenter EEG (version 3.1.4., Clinical Science Systems). We established both signal and statistical analyses by using MATLAB (version 2022b, MathWorks). The EEG-data was delivered in ‘edf’ format files. These EEG-files were imported into MATLAB using MATLAB-files created by Clinical Science Systems. We validated the statistical analysis implementations in MATLAB using IBM SPSS Statistics (version 18.0.1.0, International Business Machines Corporation) by comparing results of some datasets.

3. Questionnaires

3.1 Head Injury Symptom Checklist

The Head Injury Symptom Checklist (HISC) is a questionnaire which evaluates the presence of symptoms after TBI. The HISC addresses 19 common complaints after TBI including physical (such as headache), cognitive (forgetfulness), and emotional (anxiety) complaints. Two of the 19 complaints, itchiness and dry mouth, are non-posttraumatic and can be used to assess a patient's tendency to complain. All complaints are scored at a pre-trauma and current post-trauma status. The patients can score every complaint from 0 to 2: 0 – never, 1 – sometimes and 2 – often. We dichotomised these scores into 1 if the frequency of complaints increased and 0 if no increase happened. The end-score of the HISC is the summation of all separate complaint-scores [48,49]. For a list of symptoms that are addressed in the HISC, see Table 1. See Appendix 1 for the full Dutch HISC.

Table 1. Symptoms addressed in the Head Injury Symptom Checklist [48].

HISC-Symptoms		
Headache	Forgetfulness	Dry mouth
Dizziness	Poor concentration	Neck pain
Balance disorder	Slowness	Neck stiffness
Tinnitus	Irritability	Arm pain
Hearing loss	Noise intolerance	Itching
Increased need for sleep	Alcohol intolerance	
Fatigue	Anxiety	

3.2 Glasgow Outcome Scale – Extended

The Glasgow Outcome Scale – Extended (GOS-E) is a tool for assessing outcome after TBI. The predecessor to the GOS-E, the GOS, had five categories of outcome, ranging from 1 – dead to 5 – good recovery. The GOS-E version was proposed to increase sensitivity and is widely used (both clinically and for research purposes) to record outcome after mTBI. The scale ranges from 1 (death) to 8 (upper good recovery), and is explained in detail in Table 2 [50]. See Appendix 1 for the full Dutch GOS-E.

Table 2. Explanation of the eight-point Glasgow Outcome Scale – Extended. Adapted from Wilson et al. [50].

GOS-E 8-point scale	Domain	Criteria
1. Dead		
2. Vegetative State	Consciousness	
3. Lower SD	Function in home	Unable to look after themselves for 8 h
4. Upper SD	Function in and outside home	Unable to look after themselves for 24 h or unable to shop or unable to travel
5. Lower MD	Work/Study Social and leisure activities Family and friendships	Unable to work/study or unable to participate or constant problems
6. Upper MD	Work Social and leisure activities Family and friendships	Reduces work capacity or participation much less or frequent problems
7. Lower GR	Social and leisure activities Family and friendships Symptoms	Participate a bit less or occasional problems or some symptoms affecting daily life
8. Upper GR		No problems

4. Electroencephalography recordings

According to the EEG recording protocol, the patients sat idle and were asked to keep their eyes closed for about two minutes, followed by two minutes having their eyes opened, after which both sessions were repeated once. However, different EEG-operators often used different durations and sometimes did not repeat the process. In six acute and four subacute cases, only one pair of epochs could be identified and considered suitable.

4.1 Epoch timings

We manually determined the eyes open and closed epoch timings in the patient group EEGs. All EEG-files included annotations created by the EEG-operators. We used NeuroCenter EEG software for inspecting these EEGs and annotations. Although the annotations were not always reliable, they gave a rough idea of the epoch timings. We inspected the EEG signals for two reasons: locate eyes open and closed epochs and localise undesired artifacts. To locate the eye epochs, we used a bipolar setting (Po2) to inspect for alpha waves, which are correlated with closed eyes, and eye blinking artifacts [51,52]. We used a monopolar setting (G19) to inspect for undesired artifacts. Based on the annotations, alpha waves, blinking artifacts and other artifacts we determined the eyes open and eyes closed epochs. If possible, we determined two as long as possible epochs per eye state in every EEG-file. If no two epochs per eye state were available, we determined one epoch per eye state. We made sure the epochs did not include (major) undesired artifacts and were at least 30 seconds long, otherwise the available data may be insufficiently long. Two of the signal analyses techniques used, had their window settings set at 10 seconds with 50% overlap. A 30 second epoch therefore results in five windows, which is considered to be the lowest amount of windows needed. Of all patient measurements we included, 39 had four suitable epochs and 10 had two epochs.

We did not manually determine the timings of the eyes open and closed epochs in the healthy EEG-files. The existing annotations in the EEG-files were consistent in indicating the starts of eye open epochs and eyes closed epochs. Per EEG-file, we selected the two longest eye epochs per eye state by automatically locating the previously mentioned annotations. We corrected the epochs by cutting 5 seconds from start and end. A final automated check ensured the eye epochs were at least 50 seconds long.

5. Signal processing

5.1 Preprocessing

We inspected the patient data for visual artifacts, which were excluded (see 4.1 Epoch timings). Apart from excluding visual artefacts, no further preprocessing was deemed necessary, due to the choice of signal analysis techniques and used frequency settings. The signal analysis techniques we used relied on power spectral density and coherence estimations, in which we could analyse in accordance with frequency bands to our choice. All frequency bands we used are within the range of 1 to 30 Hz. Therefore we could eliminate important causes of artifacts like DC-offset (< 1 Hz) and power-grid interference (50 Hz).

5.2 Relative power

The first approach in signal analysis was about determining the power of EEG signals within specific frequency bands. These powers were relativised to the power of the combined bandwidth of all used frequency bands. The used frequency bands, theta, alpha and beta, as defined by Tatum [53], are described in Table 3 and visualised in Figure 1. An important reason we did not use lower frequency bands, such as delta, was to prevent DC-offset interference. Powers within higher frequency bands, such as gamma, are low. Higher frequency bands may therefore have too little information to reliably analyse. We analysed the

'eyes open' and 'eyes closed' epochs separately. In case a measurement had two epochs of both eye states, we averaged the results of these separate epochs into one 'eye open' and one 'eye closed' set of results.

Table 3. The frequency bands (as described by Tatum [53]) which we used in the relative power and power variability approaches.

Frequency band name	Frequency band range (Hz)
Theta	3.5 – 8
Alpha	8 – 13
Beta	13 –30

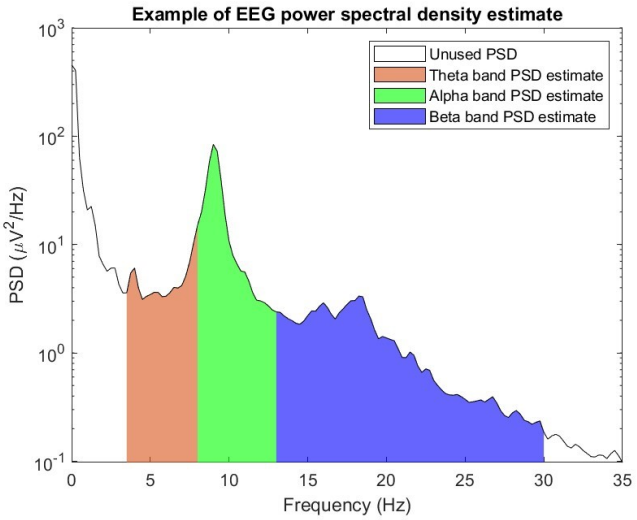

Figure 1. Power spectral density (PSD) estimate of some EEG-data. Parts of the PSD representing theta, alpha and beta bands are marked.

First, we calculated the absolute powers. Per measurement and per lead, we cut the data into sections in accordance with the eyes open or closed epochs. Per data segment a power spectrum was created using the Welch's method (3 second Hamming window with 50% overlap). Then, per frequency band, we calculated the absolute power AP as the area under the curve. This area was calculated by using a Riemann sum:

$$AP = \sum_{f_{cl}}^{f_{cu}} P_{xx}(f)\Delta f \qquad (1)$$

in which f_{cu} is the upper cut-off frequency, f_{cl} is the lower cut-off frequency and $P_{xx}(f)$ represents the power spectrum values per frequency f. The Δf (which is inverse related to the frequency resolution) was 0.25 Hz in case of the patient recordings and 0.1221 Hz in case of the control population recordings (due to the different sample frequencies of 512 and 250 Hz respectively). The cut-off frequencies are in accordance to the earlier mentioned frequency bands. We calculated the overall power as the area in between the lowest cut-off frequency of the lowest band and the highest frequency of the highest band (3.5 and 30 Hz respectively). The relative power was calculated by dividing the power of one frequency band by the overall power.

5.3 Variability of power

We determined the variability of power by calculating the variance. The first step was to calculate an array of power values per patient per situation, that is to say per frequency band, per eye state, per lead (for example for patient 1, acute phase, alpha band, eyes open, Fp1-lead). We divided every data segment in 10 second long windows with 50% overlap. At every window, we calculated the theta, alpha and beta powers like in the relative power approach. In this case however, we used the fast Fourier transform instead of the Welch's method due to the short windows, and we did not relativised the powers. Each power value is stored in the previously mentioned power value arrays. We combined the arrays of the eyes open and eyes

closed into one array so that the variability of eyes open and closed together could be determined. The variance is calculated as follows:

$$\sigma^2 = \frac{1}{N}\sum_{i=1}^{N}(x_i - \mu)^2 \quad \textbf{(2)}$$

in which N is the power value array size, μ the mean of the array and x_i the individual power values.

5.4 Power symmetry

To calculate the power symmetry, first we calculated the power of EEG signals at the frequency band of 1 – 25 Hz. This frequency band is in accordance with the original Brain Symmetry Index [32]. Given a measurement had two epochs of both eye states, we first averaged the powers of the two matching epochs. Per symmetric oriented lead pair, the power symmetry PS was calculated as the absolute value of the relative power difference:

$$PS = \frac{|PL - PR|}{PL + PR} \quad \textbf{(3)}$$

in which PL is the power at the left lead and PR the power at the right lead. EEG-data from the leads at the centre line are not taken into account, since these are lagging a symmetric counterpart. See Table 4 for an overview of the lead-signal-pairs.

Table 4. Lead-signal-pairs used in the power symmetry approach.

Left lead	Right lead
Fp1	Fp2
F3	F4
F7	F8
C3	C4
T3	T4
P3	P4
T5	T6
O1	O2

5.5 Coherence

Coherence was calculated in between neighbouring and symmetric oriented lead-signal-pairs. For an overview of lead-signal-pairs, see

Table 5. We set the MATLAB coherence function to use 10 second windows with 50% overlap. It provides an array as output representing coherence levels at different frequencies. We only used coherence values representing the range 3.5 – 30 Hz (which is the combination of the theta, alpha and beta band). These values were averaged. In case a measurement had two epochs of both eye states, we averaged the results of these separate epochs into one ‘eye open’ and one ‘eye closed' set of results.

Table 5. The fifty-eight lead-signal-pairs used in the coherence approach. Every 'X' marks a combination.

Leads	Fp1	Fp2	F7	F3	Fz	F4	F8	T3	C3	Cz	C4	T4	T5	P3	Pz	P4	T6	O1
O2															X	X	X	X
O1													X	X	X			
T6											X	X	X			X		
P4										X	X	X		X	X			
Pz									X	X	X			X				
P3								X	X	X			X					
T5								X	X									
T4						X	X	X			X							
C4					X	X	X		X	X								
Cz				X	X	X			X									
C3			X	X	X			X										
T3			X	X														
F8		X	X			X												
F4		X		X	X													
Fz	X	X		X														
F3	X		X															
F7	X																	
Fp2	X																	

6. Phase differences

To take into account the development in between phases, we analysed the differences in between phase results as well. The acute phase results are subtracted from the subacute phase results per situation per patient (given data from both phases is available).

7. Divergency selection

mTBI is a heterogeneous disorder: patients acquire injury at different sites at the scalp and therefore EEG signals at different leads may be altered differently. We had to design our methods with this heterogeneity in mind. Another challenging aspect was the large number of datasets that could potentially be statistically compared, as a result of using different signal analyses approaches, phases, frequency bands and eye states. In total, 909 datasets could be compared to both HISC scores and GOS-E outcomes. For a full explanation on this number, see Appendix 2. This high number would potentially jeopardise the significance of the statistical analyses in this study. Therefore, we aimed to reduce the amount of statistical analyses, while also keeping the heterogeneity in mind.

To both reduce the number of datasets and also correct for heterogeneity, we designed an algorithm we called the 'divergence-selection-algorithm'. We applied this algorithm in all four approaches. Per approach, we did not use all data of all lead-signals or lead-signal-pairs. Instead, given a certain situation (that is, given a certain patient, phase, frequency band and eye state) we picked out the most divergent lead-signals or lead-signal-pairs (depending on the approach) by comparing to the healthy control population average HA. We relativised the results of the signal analysis Res to these averages, giving a relative result $RelRes$:

$$RelRes = \frac{Res\ - HA}{Res\ + HA} \qquad (4)$$

Given a certain patient and situation (based on phase, frequency band and eye state) a set of relative results represents the original results of all different leads or lead-pairs. We picked out the two results deviating most from the healthy population average (the lowest and highest relative results). We repeated this process for all patients. Therefore, instead of having a dataset for every lead-signal or lead-signal-pair given a certain situation, we created two data sets (one with lowest divergence values and one with highest divergence values). To determine the population averages of the control group, we also applied all signal analyses approaches to the control group EEG-data. Per situation (given a certain patient, phase, frequency band, eye state and lead-signal(-pair)) the average of the control group was calculated.

We applied the divergence-selection-algorithm as just described to acute and subacute data. A similar algorithm is applied to the results of the phase differences, although in this case we did not relativised the phase-difference-results to healthy group averages. The picked-out values are the highest and lowest difference values. Not that in the same patient in different phases, different leads could be selected. After the divergence-selection-algorithm has been applied to all four approaches, 78 datasets were generated. See Appendix 2 for an explanation on this number.

For a detailed example of the entire signal analysis and divergence-selection-algorithm process, see Appendix 4.

8. Statistics

We analysed the results of the signal analysis approaches twice, once in comparison with the HISC scores and once in comparison with the GOS-E outcomes. Since the population is small, we did not consider multivariable testing to be a proper approach, therefore all testing was restricted to univariable testing. Due to the explorative nature of this research, we only considered statistical comparison with significance values smaller than 0.01 to be significant.

8.1 HISC scores

Because of the explorative nature of this research, we considered linear regression not to be a suitable option to test the signal analysis data in comparison to the HISC scores. Therefore, we calculated correlation values. First, we tested the HISC scores and the logarithmic transform of the HISC scores of all patients for normality. Via a Shapiro-Wilk test the hypothesis, that (the logarithmic of) the HISC scores are normally distributed, was rejected ($p = 0.001$ and $p < 0.001$, latter logarithmic). Since the HISC data was not normally distributed, we applied the non-parametric Spearman's rank correlation coefficient test, which is suitable for non-normal distributed input data. The correlation scores vary in between -1 and 1; a score close to 0 suggests little correlation, a scores close to -1 or 1 suggests a profound correlation.

8.2 GOS-E outcomes

We transformed the scores of the GOS-E into binary outcomes. We labelled scores of 7 or lower as a poor outcome and scores of 8 as a good outcome, in accordance with literature [54].

We split every dataset into a good and a poor GOS-E outcome subset. We tested these subsets, as well as their logarithmic transforms for normality (see Table 6 more details). In many datasets, the results of these subsets turned out to be not normally distributed. Therefore, for sake of consistency, we used a Mann-Whitney U test in further statistical analyses for all datasets to test for a significant difference in between the groups.

Table 6. Overview of the amount of datasets that, according to the Shapiro-Wilk test were normally distributed, considering a significance value threshold of 0.05. These datasets were created by the divergence-selection-algorithm after applying the signal analyses. # – Absolute number, % – Relative number in percentage.

	Relative power		Power variability		Power symmetry		Coherence	
	#	%	#	%	#	%	#	%
Acute	0	0.0	1	8.3	0	0.0	0	0.0
Acute logarithmic	11	45.8	4	33.3	3	37.5	2	25.0
Subacute	2	8.3	5	41.7	1	12.5	0	0.0
Subacute logarithmic	14	58.3	6	50.0	3	37.5	2	25.0
Phase difference	1	4.2	6	50.0	2	25.0	0	0.0
Phase difference logarithmic	6	25.0	0	0.0	1	12.5	0	0.0

Results

1. Population characteristics

We initially included 31 patients. We excluded one patient because of missing all EEG-data and five because of missing questionnaire data. Of the 26 remaining patients (average age of 47.9 ± 16.8 years), we proceeded to analyse the acute EEG-data of 23 patients (average age of 48.7 ± 16.5 years) due to data-loss. Subacute EEG-data was available from all 26 patients. The average age of the control group, which had a size of 120, was 46.5 ± 18.1 years. For an overview of the population characteristics, see Table 7.

Table 7. Population characteristics of the participants in this study. All acute phase (mTBI-A) patients are included in the subacute (mTBI-S) population.

	mTBI-A (n = 23)	mTBI-S (n = 26)	Control (n = 120)
Average age (years) ± SD	48.7 ± 16.5	47.9 ± 16.8	46.5 ± 18.1
Male/female	14/9	14/12	63/57
Abnormal CT scan	48%	46%	-
Medication	39%	35%	-
Questionnaire results			
Average HISC ± SD	4.5 ± 5.0	4.3 ± 4.8	-
Good/poor GOS-E	12/11	13/13	-
TBI causes			
Bicycle accident	57%	54%	-
Motor accident	9%	8%	-
Fall	22%	19%	-
Other	9%	12%	-
Unknown	4%	8%	-

2. HISC scores and GOS-E outcomes

When comparing the HISC scores and GOS-E outcomes, high HISC scores (> 4) correlate with a poor GOS-E outcome and a low HISC score usually implies a good GOS-E outcome (see Figure 2). Both the HISC scores and logarithmic transformed HISC scores were not normally distributed (tested with a Shapiro-Wilk test, P = 0.001 and P < 0.001 respectively).

3. HISC scores comparison results

When comparing the signal analysis datasets to the questionnaire results, no statistical significant comparisons were found, considering a significance value threshold of 0.01. In comparison to the HISC, five out of the 78 datasets showed a significance value smaller than 0.1 and an absolute correlation value larger than 0.3. These comparisons are reported below. For an overview of these five comparisons, see Table 8. For a complete overview of all comparison results, see appendix 5.

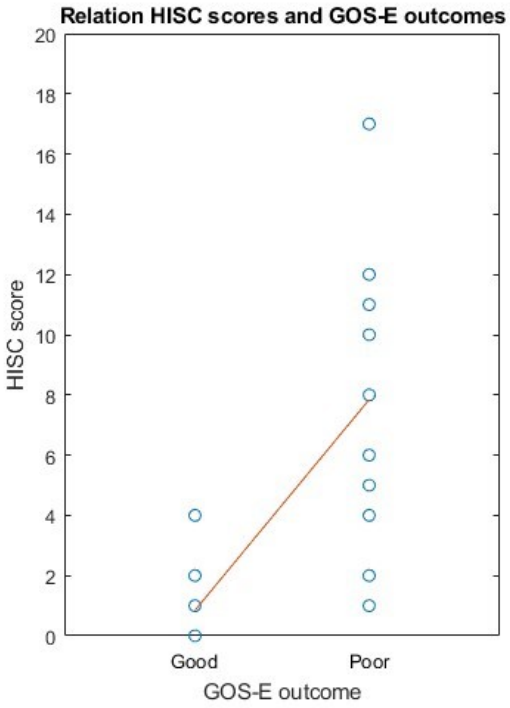

Figure 2. Visual comparison between the HISC scores and the GOS-E outcomes. HISC scores of five and higher are exclusively found in patients with a poor GOS-E outcome. HISC scores of four and lower are mostly found in the good GOS-E outcome patients.

Table 8. Overview of the reported Data-HISC scores statistical comparisons. All have absolute correlation values larger than 0.3 and significance values smaller than 0.1. RP – relative power, PV – power variability, PS – power symmetry.

Approach	Phase	Band	Divergence	Eye state	Correlation	Significance	Paragraph
RP	Difference	Alpha	Highest	Closed	-0.43	0.04	3.1
PV	Subacute	Theta	Highest	-	-0.43	0.03	3.2
PS	Difference	-	Highest	Open	-0.37	0.08	3.3
PS	Acute	-	Highest	Closed	0.36	0.09	3.4
PS	Subacute	-	Lowest	Open	-0.34	0.09	3.5

3.1 Relative power and HISC

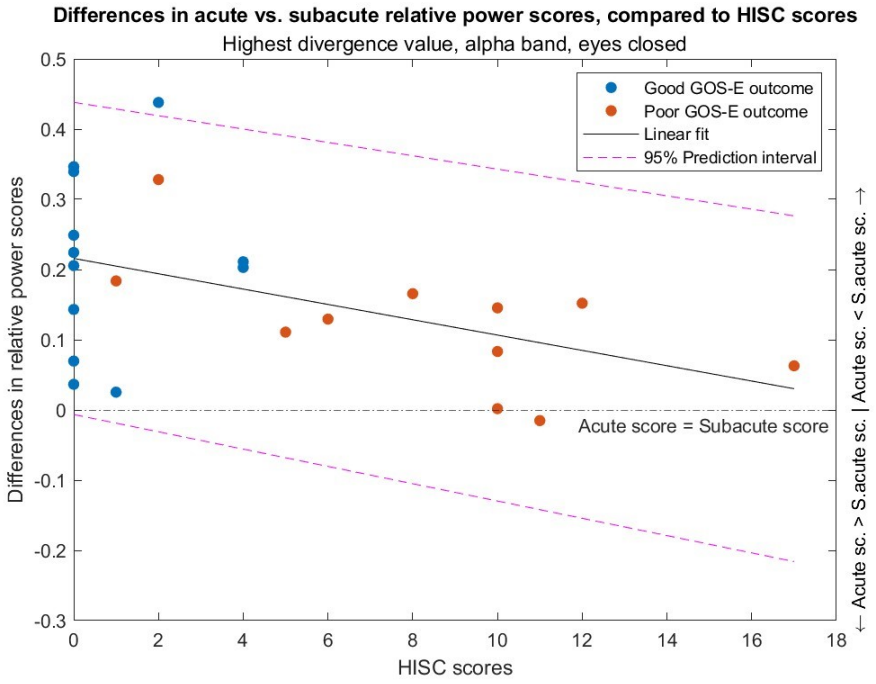

Figure 3. Comparison between the HISC scores and the relative power, phase difference, high divergence values, alpha band, eyes closed dataset. The Spearman's rank correlation coefficient test resulted in a correlation score of -0.44 and a significance value of 0.04, making this comparison the best scoring HISC score comparison. Acute sc. – acute score, S.acute sc. – subacute score.

In comparison to the HISC scores, the relative power, phase difference, alpha band, eyes closed, highest divergence values dataset scores a correlation value of -0.44 and a significance of 0.04 and shows a negative trend (see Figure 3). Patients with high HISC scores (more persistent complaints) tend to have similar relative alpha power scores in the acute and subacute phase, while patients with low HISC scores (less or no persistent complaints) have higher relative alpha powers in the subacute phase, considering the eyes closed measurements and the high divergency values.

3.2 Power variability and HISC

The power variability, subacute phase, theta band, highest divergence values dataset scores, in comparison to HISC scores a correlation value of -0.43 and a significance of 0.03. Patients with higher HISC scores tend to have lower theta power variability than healthy average (see Figure 4). Patients scoring low on the HISC tend to have scores above or around healthy average.

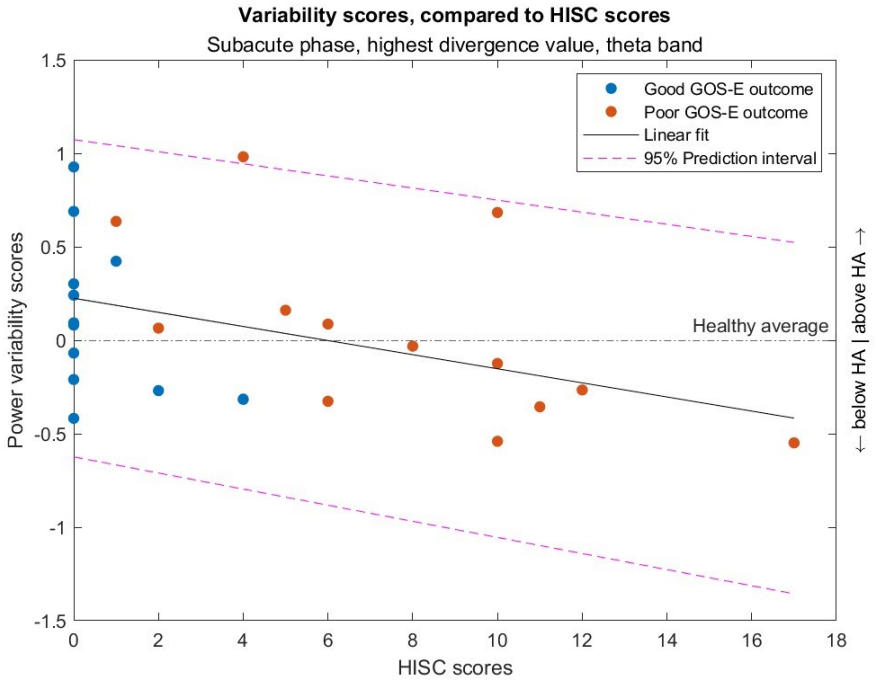

Figure 4. Comparison between the HISC scores and the power variability, subacute phase, high divergence values, theta band dataset. The Spearman's rank correlation coefficient test resulted in a correlation score of -0.43 and a significance value of 0.03. HA – healthy average.

3.3 Power symmetry and HISC – phase differences

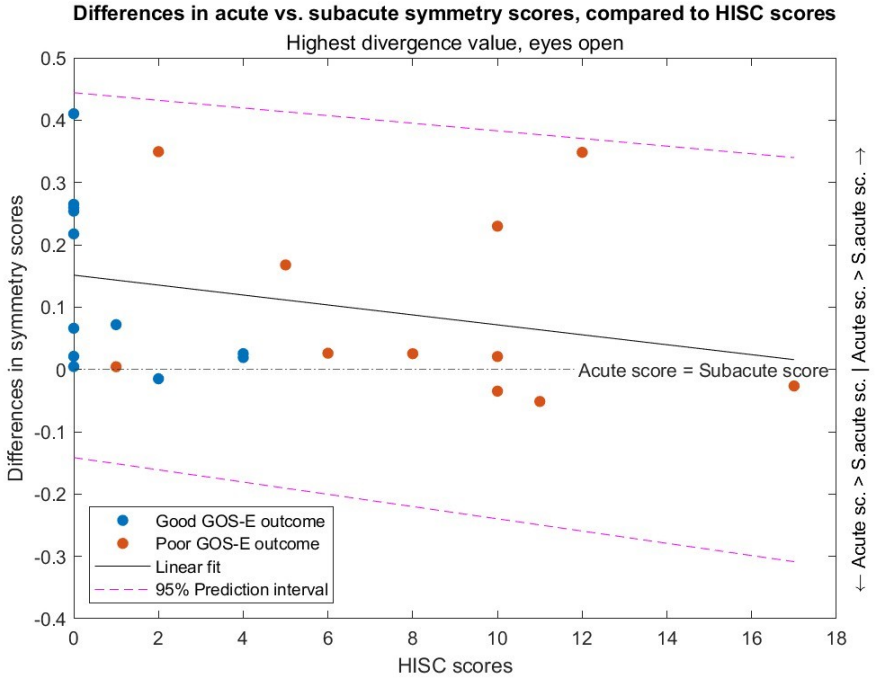

Figure 5. Comparison between the HISC scores and the power symmetry, phase difference, high divergence values, eyes open dataset. The Spearman's rank correlation coefficient test resulted in a correlation score of -0.37 and a significance value of 0.08. Acute sc. – acute score, S.acute sc. – subacute score.

In comparison to the HISC scores, the power symmetry, phase difference, eyes open, highest divergence values dataset scores a correlation value of -0.37 and a significance of 0.08. Symmetry scores of high HISC scoring patients tends to be comparable in both phases. Patients with low HISC scores tend to have higher symmetry scores (i.e. less symmetric EEG) in the subacute phase (see Figure 5). This dataset only considers the most asymmetric lead-pair per patient.

3.4 Power symmetry and HISC – acute phase

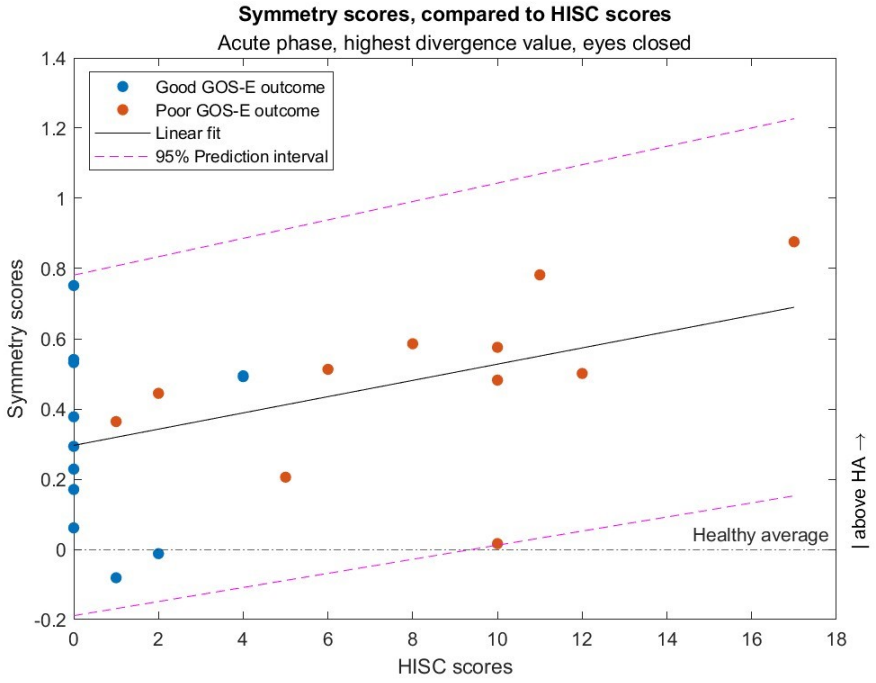

Figure 6. Comparison between the HISC scores and the power symmetry, acute phase, high divergence values, eyes closed dataset. The Spearman's rank correlation coefficient test resulted in a correlation score of -0.36 and a significance value of 0.09. HA – healthy average.

The power symmetry, acute phase, eyes closed, highest divergence values dataset scores, in comparison to the HISC, a correlation value of 0.36 and a significance of 0.09. Patients with lower HISC scores tend to have lower symmetry scores (display a more symmetric EEG) than the patients with higher HISC scores. Almost all patients score higher (less symmetric) than healthy average (see Figure 6). Like in the previous dataset, this dataset only considers the most asymmetric lead-pair per patient.

3.5 Power symmetry and HISC – subacute phase

The final HISC comparison addressed in this chapter is the power symmetry, subacute phase, eyes open, lowest divergence values dataset. It scores a correlation value of -0.34 and a significance of 0.09. After plotting, the comparison seems inconclusive (see Figure 7), considering the low angle of the trendline compared to the vertical spread of the datapoints. These scores, which are only based on the most symmetric lead-pair per patient, seem to be lower (and thus more symmetric) than the healthy population averages.

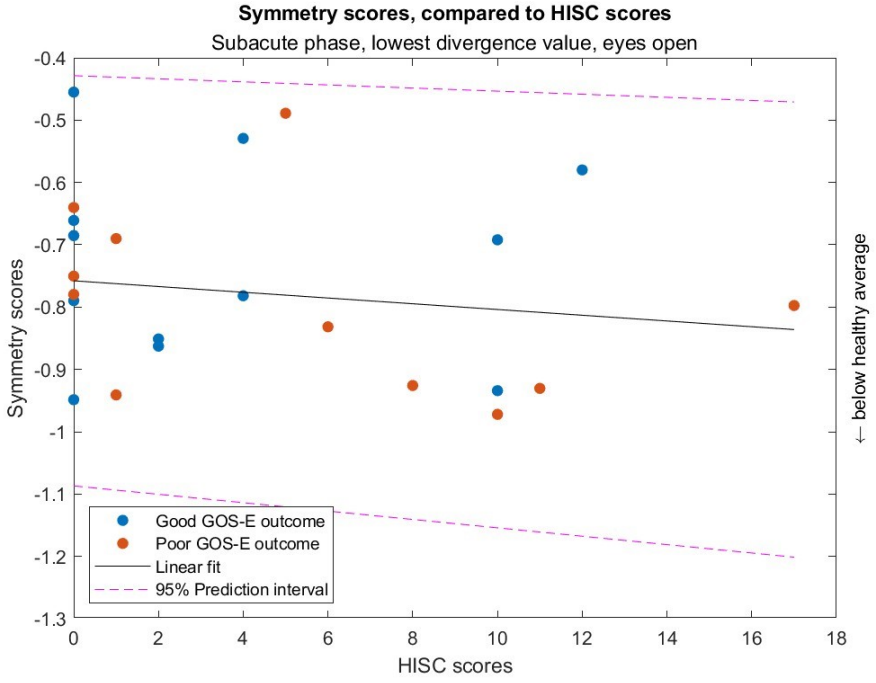

Figure 7. Comparison between the HISC scores and the power symmetry, subacute phase, low divergence values, eyes open dataset. The Spearman's rank correlation coefficient test resulted in a correlation score of -0.34 and a significance value of 0.09. Due to the low angle of the trendline compared to the vertical spread of the datapoints, the correlation may be considered inconclusive.

4. GOS-E outcomes comparison results

Of all 78 datasets that were statistically compared to the GOS-E outcomes, four were considered for further analysis. Only these comparisons scored significance values smaller than 0.1. For an overview of these four comparisons, see Table 9Table 8. For a full overview of all comparisons, see appendix 5.

Table 9. Data-GOS-E outcomes statistical comparisons considered to be of interest. All have significance values smaller than 0.1. Coh – Coherence, RP – relative power, PS – power symmetry.

Approach	Phase	Band	Divergence	Eye state	Significance	Paragraph
Coh	Acute	-	Lowest	Open	0.04	4.1
RP	Difference	Alpha	Highest	Closed	0.08	4.2
Coh	Acute	-	Lowest	Closed	0.08	4.3
PS	Subacute	-	Lowest	Open	0.09	4.4

4.1 Coherence and GOS-E – open eyes

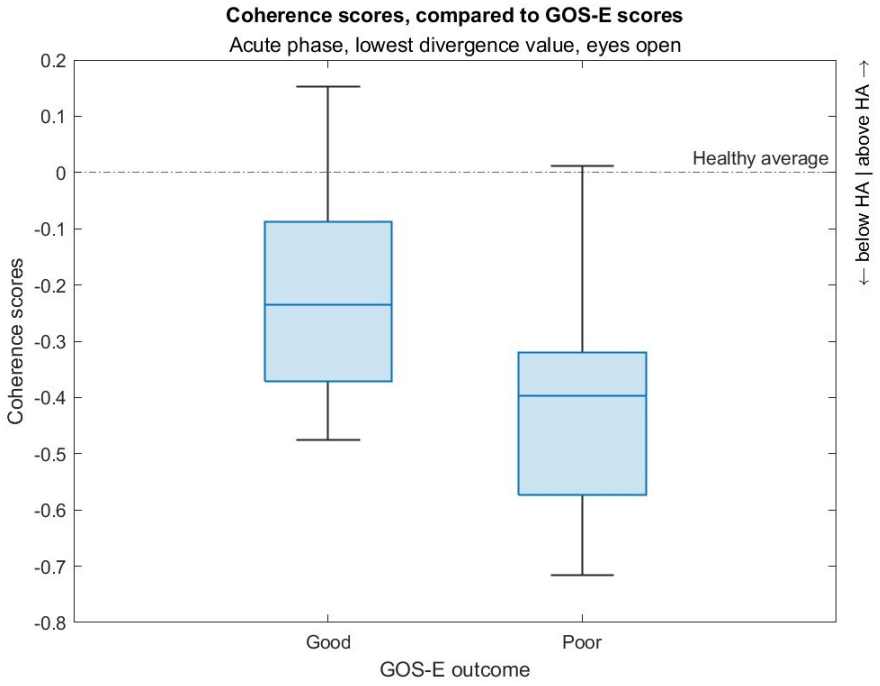

Figure 8. Comparison between the GOS-E outcomes and the coherence, acute phase, low divergence values, eyes open dataset. The Mann-Whitney U test resulted in a significance value of 0.04, making this comparison the best scoring GOS-E outcome comparison. Acute sc. – acute score, S.acute sc. – subacute score.

In comparison to the GOS-E outcomes, the coherence, acute phase, eyes open, lowest divergence values dataset has a significance value of 0.04. Both patient groups tend to have coherence scores below the healthy average, with the poor outcome group scoring lower (see Figure 8). All coherence values below -0.5 are exclusively found in the poor outcome group. This comparison only takes the least coherent lead-pair per patient into account.

4.2 Relative power and GOS-E

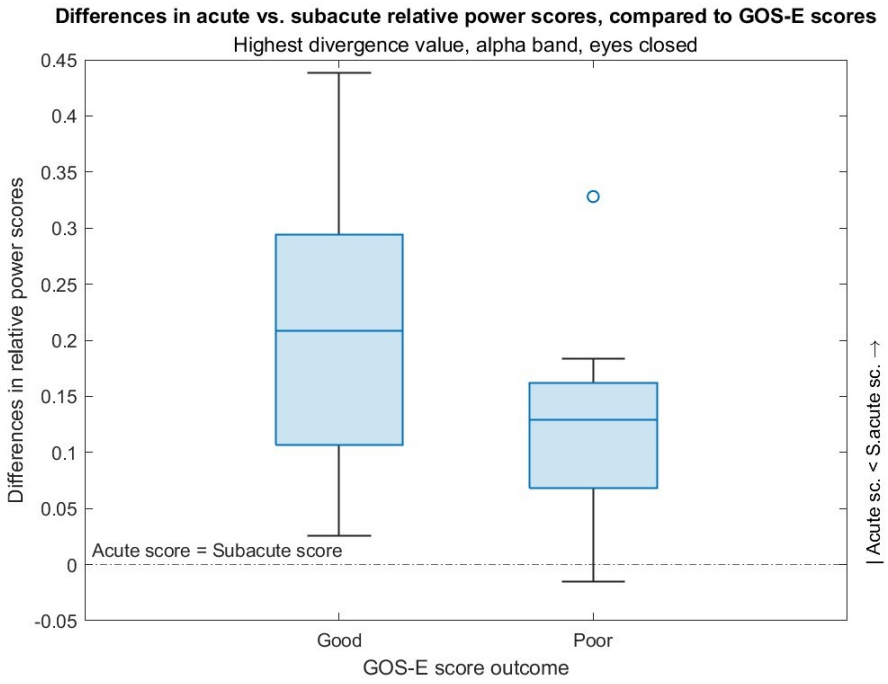

Figure 9. Comparison between the GOS-E outcomes and the relative power, phase difference, high divergence values, alpha band, eyes closed dataset. The Mann-Whitney U test resulted in a significance value of 0.08. HA – healthy average.

The relative power, phase difference, alpha band, eyes closed, highest divergence values dataset comparison scores a significance value of 0.08. The comparison between this dataset and the HISC scores is described earlier (see paragraph 3.1). According to the comparison to the GOS-E outcomes, almost all patients have a higher relative alpha powers in the subacute phase than in the acute phase (see Figure 9). In the good GOS-E outcome group, these differences tend to be larger than in the poor outcome group. Difference values of larger than 0.2 are almost exclusively found in the good outcome group. This dataset only considers the highest scoring lead per patient, i.e. the lead with the largest relative power difference.

4.3 Coherence and GOS-E – closed eyes

The coherence, acute phase, eyes closed, lowest divergence values dataset scores a significance value of 0.08 in comparison to the GOS-E outcomes. The poor outcome group has all its coherence scores below average (see Figure 10). The good outcome group has its scores mostly below health average. The average good outcome group score is not as low as the average poor outcome group score. This comparison only takes the lowest coherence scoring lead-pair per patient into account.

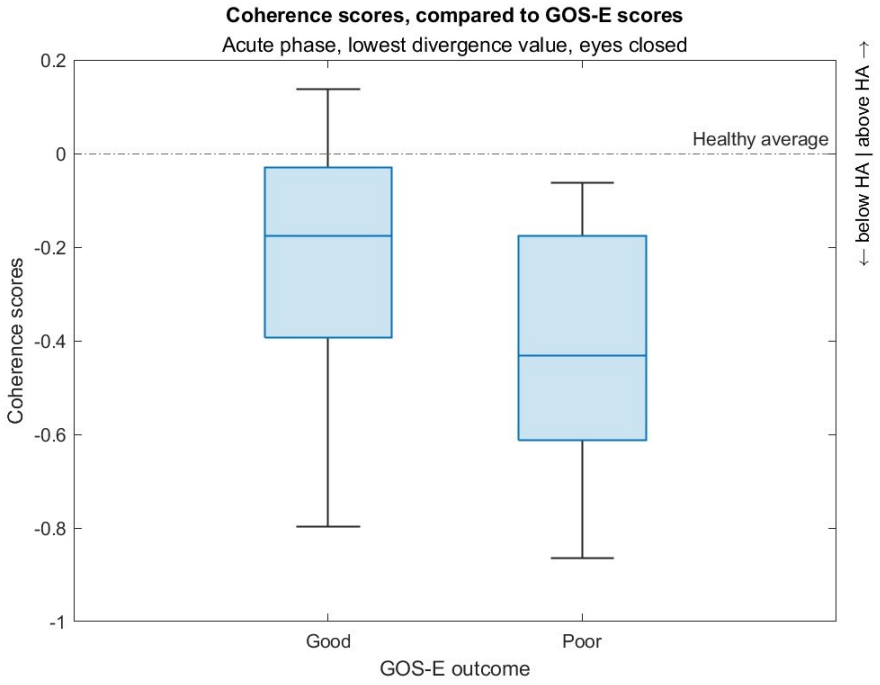

Figure 10. Comparison between the GOS-E outcomes and the coherence, acute phase, low divergence values, eyes closed dataset. The Mann-Whitney U test resulted in a significance value of 0.08. HA – healthy average.

4.4 Power symmetry and GOS-E

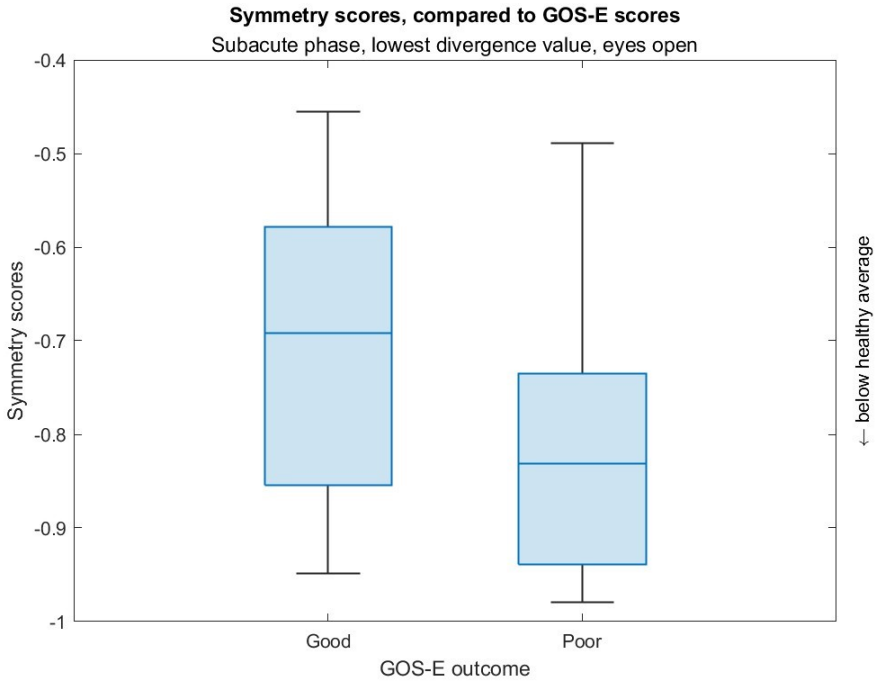

Figure 11. Comparison between the GOS-E outcomes and the power symmetry, subacute phase, low divergence values, eyes open dataset. The Mann-Whitney U test resulted in a significance value of 0.09.

The last dataset that is addressed in this chapter is the power symmetry, subacute phase, eyes open, lowest divergence values dataset. In comparison to the GOS-E outcomes, it scores a significance value of 0.09. The comparison suggests that patients within the poor outcome group tend to have lower symmetry scores, i.e. higher level of symmetry, than those from the good outcome group. (see Figure 11). Overall, all patients score lower (have higher levels of symmetry) than the healthy average. These scores are only based on the most symmetric lead-pair per patient.

5. Overview results comparisons

Table 10 and Table 11 provide an overview of the above described results. The result addressed in paragraph 3.5 is not included, considering the inconclusive correlation.

Table 10. Overview of the top four scoring HISC score comparisons and their possible implications for mTBI patients, based on HISC score comparisons. For more details about the comparisons and the specific settings to which these implications apply, see paragraph 3. Par. – Paragraph, Res.# – result number, Cor. – correlation value, P – significance value.

Par.	Summarised implications of HISC comparisons	Cor.	P
3.1	Patients with fewer complaints have lower relative alpha power in the acute phase compared to the subacute phase.	-0.44	0.04
3.2	Subacute patients with more complaints have lower theta power variability than the healthy average.	-0.43	0.03
3.3	Patients with fewer complaints have a less symmetric EEG in the acute phase compared to the subacute phase.	-0.37	0.08
3.4	Acute patients have a less symmetric EEG than healthy controls. Those with more complaints have a less symmetric EEG compared to those with few complaints.	0.36	0.09

Table 11. Overview of the top four scoring GOS-E outcome comparisons and their possible implications for mTBI patients, based on GOS-E outcome comparisons. For more details about the comparisons and the specific settings to which these implications apply, see paragraph 4. Par. – Paragraph, Res.# – result number, P – significance value.

Par.	Summarised implications of GOS-E comparisons	P
4.1	Acute patients have a lower coherence than healthy controls. Those with a poor outcome have a lower coherence compared to those with a good outcome.	0.04
4.2	Patients have higher relative alpha powers in the subacute phase than in the acute phase. Differences are larger in those with a good outcome compared to those with a poor outcome.	0.08
4.3	Acute patients have a lower coherence than healthy controls. Those with a poor outcome have a lower coherence compared to those with a good outcome.	0.08
4.4	Subacute phase patients have a more symmetric EEG than healthy controls. Those with a good outcome have a less symmetric EEG compares to those with a poor outcome.	0.09

Discussion

In this explorative study we searched for correlations between EEG characteristics and outcome after mild traumatic brain injury. These EEG characteristics included relative power, power variability, power symmetry and coherence. We used a self-designed algorithm to select the most abnormal lead or lead-pairs per patients to both account for the heterogeneity among patients and reduce the amount of statistical comparisons. Several interesting trends were identified, which are discussed below.

The first trend implies that patients with few or no persistent complaints tend to have a higher relative alpha power in the subacute phase than in the acute phase, while patients with many persistent complaints tend to have a similar relative alpha power in both phases (correlation value = -0.44, P = 0.04). Literature suggest that TBI patients have reduced absolute alpha powers compared to healthy individuals [34,39]. Our findings suggest that patients with fewer complaints recover from a reduced to a normal alpha power in the first weeks after trauma. Such a recovery seems absent in patients with more persistent complaints. Previous studies suggested that the reduction in alpha power is caused by a reduced cortical excitability [39]. Acute reduction in excitability is linked to a neurometabolic cascade involving an efflux of potassium, release of amino acids, increase of glycolytic rates, accumulation of calcium and a reduction in cerebral blood flow [55]. We speculate that patients with a poor recovery from this reduced excitability state develop persistent complaints, and may be identified using EEG.

Second, we found a trend that implies that patients with many persistent complaints have a lower theta power variability than the average of the healthy controls, while patients with few or no persistent complaints have a theta power variability comparable to or higher than healthy average (correlation value = -0.43, P = 0.03). This is in contradiction with the study from Williams et al. [40], which showed that mTBI patients had a higher theta power variability than controls. However, it must be noted that this particular study was focused on insomnia and had a small population of nine patients. Kaltiainen et al., who used a setting more comparable to ours, showed a major increase in spontaneous theta activity in seven out of twenty-seven mTBI patients [56]. The cause of this abnormal theta band activity is unknown. It may be related to changes in deep midline structures, to slowing of physiological alpha activity or to axonal damage causing a mild form of polymorphic delta activity [57].

Last, we identified a trend that all mTBI patients have lower coherence scores than the average of the healthy controls, and poor recovered patients have even lower coherence scores than well recovered patients (P = 0.04). Previous studies on coherence after mTBI report contradictory results and disagree on whether the coherence increases or decreases after mTBI [39,47,58]. Lewine et al. [59] suggested that a decrease in interhemispheric beta coherence may reflect callosal integrity and we suggest that it is plausible that the decrease in coherence in our result has a similar cause. If true, our result may suggest that poor recovering patients have a poorer callosal integrity compared to good recovering patients. However, since our selection-algorithm does not necessarily select interhemispheric lead-pair data, this suggestion is at most plausible.

Strengths and limitations

A strength of our study is that it is a prospective study with well-defined and clear inclusion and exclusion criteria. Some may consider the population size of this study (23 or 26, depending on phase) to be small. Yet, considering the explorative nature of this study, we consider the population size to be appropriate.

With regards to age and gender, our patient population is comparable to other Dutch mTBI cohorts [11,60–62]. All patients in our cohort were admitted to hospital for observation, whereas in the entire mTBI population most patients are either discharged from the emergency department or not admitted to the

emergency department at all [2]. Therefore, it might be argued that our cohort is at a more sever end of the mTBI spectrum, making the results of our study not extrapolable to the entire mTBI population.

To make sure that the healthy group is representable to the patient group, the average age and male/female ratio were matched. Because all the healthy group individuals were patients at the outpatient clinic, it could be argued that the healthy group was not fully representative to a real healthy population. However, after assessment of their EEGs by medical professionals, their EEGs were judged to be normal. Therefore it is deemed acceptable to use these EEGs as healthy EEGs for their use in this study.

Measuring the same patients in both acute and subacute phase is rather uncommon and provides interesting insights. The EEG measurements themselves were performed by experienced personnel in a setting specifically designed for EEG measurements, using high quality equipment. Therefore the measuring quality can be considered to be well sufficient. However, the measurement protocol for this study was not always applied equally in every measurement. This was due to different operators performing the measurements and difficulties with applying the protocol in some patients in the acute phase. According to the protocol, two two-minute epochs had to be measured of both eye states. Some EEGs had only one (suitable) epoch per eye state and/or short epochs. EEGs with too short epochs (<30 seconds) were excluded. The shorter epochs may have had influence on the results of the signal analyses. It is expected that the influence on the relative power, power symmetry and coherence, is limited. The influence on power variability may be more profound, because the chance of an increase in variability within a signal increases with signal length.

The questionnaires used in this study have been validated and can therefore be considered as sufficiently reliable [48,63,64]. One disadvantage of the HISC questionnaire is that it relies on long-term memory; the patients have to score symptoms prior to their trauma, which is at least six months ago at the time of filling in the questionnaires. On one hand it is well possible that TBI effects the long-term memory of patients [65]. On the other hand patients may be effected by the 'good-old-day' bias, which is caused by the tendency of individuals to underestimate their past problems and consider themselves healthier in the past [66]. When scoring the differences between pre-injury and six months post-injury, any questionnaire will have the same dependency on the patients' long-term memory and therefore no alternative is expected to do better in this regard. The GOS-E questionnaire can be considered to be too rudimentary for mTBI research. The patients in our study scored usually 7 or 8 points and in some instances 6 points; no patient scored 5 or lower. Due to this range in scores, the sensitivity of the GOS-E is limited. However, the GOS-E is a frequently used, validated questionnaire for TBI research [64].

The divergence-selection-algorithm was important to our study, because it was a solution to two problems. On one hand, the amount of statistical comparisons had to be reduced, to limit the impact on the significance value of the individual comparisons. On the other hand, the heterogeneity of the patient population may weaken the comparison results if a per-lead or per-lead-pair method is used. Different patients suffer impact at different sites at the scalp. Therefore, it is likely that the changes in EEG also differ per patient, i.e. EEG-data at different leads are affected in different patients. A per-lead or per-lead-pair method will not use the most affected EEG-data of all patients. The divergence-selection-algorithm does pick out the most deviating data per patient and therefore likely the most affected data.

This divergence-selection-algorithm is newly created and its validation has been limited. We did validate the algorithm using self-created signals which were purposely designed for this validation and only reflect real EEG-data to a limited degree (see Appendix 3). This, however, did enable us to validate the basic functionality of the algorithm with a high degree of certainty. For full validation, a more elaborate set of tests are required, using a large amount of EEG-data with known EEG characteristics. Such an elaborate and labour intensive validation did not fit the scope of our study.

We had to make decisions on what settings to use in the signal analysis techniques. The only relevant adjustable settings of the Welch's method, used in the relative power and power symmetry approaches,

are the window shape and length. We used a Hamming window, which is commonly used in the Welch's method. We set the window length at three seconds. No other lengths were tested, for this length was, to our experience, appropriate. Finetuning the window length may have unnecessarily complicated this study and may have increased the amount of statistical comparisons (depending on the number of different window lengths used).

In the relative power and power variability approaches, the theta, alpha and beta bands were analysed separately. Within EEG analysis, separating this way is common practice, especially considering many studies focus on alpha band power [30,44,47]. Lower frequency bands were not used due to possible DC-offset interference and higher bands were not used because these bands are expected to contain little to no useful information. The coherence approach used one single bandwidth covering the theta, alpha and beta bands. We could have separated the entire bandwidth into theta, alpha and beta bands as well, but this would have come with the disadvantage of increasing the amount of statistical comparisons, which may be disadvantageous for the significance level.

We did not use the original BSI, because it does not analyse the symmetry of lead-pairs separately. Instead it first calculates the average powers of both hemispheres and then calculates the symmetry index. If a patient has a local trauma only affecting the EEG at one or two leads, it is likely it will barely have any effect on the BSI. Therefore we preferred a method in which the lead-pairs are analysed separately [67].

Ethical implications of using a prediction tool

Every year many new mTBI patients would potentially benefit from receiving preventive treatment right after acquiring mTBI. Currently it is insufficiently known which patients would benefit from such treatment. Research into correlations between chronic complaints and biomarkers, and by extension the development and application of a prediction tool, is therefore of high importance. It could however be argued that, if it is possible to predict a patients' prospect, the medical scientific community is morally obliged to look into the possibility to develop suitable treatments.

Having a prediction tool has major benefits, yet it also comes with risks. An important risk for prediction tools in general is that it may to some extent replace the judgment of medical professionals. After successful implementation, a hospital department could gradually rely more and more on the tool and could therefore neglect to give sufficient 'human' judgment. This can result in unnecessary errors introduced by the prediction tool. If errors occur, a difficult matter of responsibility may arise. The medical professionals using the tool or the manufacturers of the tool may be to blame and some could even argue that, in case of a very advanced AI tool, the tool itself can be blamed. However, when the tool is built on difficult to understand, complicated (AI) algorithms, addressing responsibility may not be straightforward.

Prospect

In our study we explored for potential correlations rather than to prove correlation between qEEG and presence of persistent complaints or lack of recovery. Future studies, preferably with larger patient populations and focused on the possible trends found, may prove or disprove these correlations. If such studies are only focussed on the setting (eye state, band, phase) and signal analysis technique in accordance to the found trends, the relative small amount of statistical comparisons may not necessitate a selection-algorithm like in our study. However, these studies will still have to deal with the heterogeneity of (the trauma of) patients. Therefore, some selection mechanism, like the divergence-selection-algorithm in our study, is still recommended.

Due to the current implementation of the divergence-selection-algorithm we did not acquire data on the effect the different impact sites in patients has on recovery or persistence of complaints. Maybe, future

studies focused on these possible effects could be valuable. It is well plausible that different impact sites have different prospects. A future study on interhemispheric coherence may also be valuable to support or disprove the idea that callosal integrity may reflect the recovery of mTBI patients.

An alternative to studies focused on validating the trends found in this study, may be a study using machine learning algorithms with the trends found in this study as input. Tewarie et al. [31] showed that, in moderate and severe TBI patients, machine learning (in this case Random Forrest) is able to find correlations using many (inconclusive) trends as input.

A category of signal analysis techniques not addressed in this study is entropy. Entropy has been used in some TBI EEG studies, yet (to our knowledge) not with a goal, method and setting comparable to our study [68–70]. Many forms of entropy exist and could be tested. One study seemed promising in predicting prognosis in severe TBI patients [70]. So, more research on entropy in mTBI can well be considered interesting.

Conclusion

Three non-significant, yet possible correlations have been found when comparing EEG characteristics of mTBI patients with and without persistent complaints and with and without good recovery. These correlations are based on the results of relative alpha power, theta power variability and coherence analyses.

Especially considering the fact that currently no proper prediction tool is available to distinguish the mTBI patients that are likely to acquire persistent complaints from the patients that will likely recover well, and considering the fact that many patients annually acquire (persistent) mTBI related complaints, more research into correlations between complaints and potential biomarkers is very important. Future research may be focused on validating the possible correlations found in our study or implementing these correlations into a machine learning system. A study comparable to ours into entropy could also be interesting.

To conclude, we found some possible correlations that may be interesting to further research in an effort to create a prediction tool to better categorise mTBI patients.

References

1. Katz DI, Cohen SI, Alexander MP. Mild traumatic brain injury. *Handb Clin Neurol*. 2015;127:131-156. doi:10.1016/B978-0-444-52892-6.00009-X
2. Cassidy JD, Carroll LJ, Peloso PM, et al. Incidence, risk factors and prevention of mild traumatic brain injury: Results of the WHO Collaborating Centre Task Force on Mild Traumatic Brain Injury. *J Rehabil Med Suppl*. 2004;(43):28-60. doi:10.1080/16501960410023732
3. Haarbauer-Krupa J, Pugh MJ, Prager EM, Harmon N, Wolfe J, Yaffe K. Epidemiology of Chronic Effects of Traumatic Brain Injury. *https://home.liebertpub.com/neu*. 2021;38(23):3235-3247. doi:10.1089/NEU.2021.0062
4. Teasdale G, Jennett B. Assessment of coma and impaired consciousness. A practical scale. *Lancet (London, England)*. 1974;2(7872):81-84. doi:10.1016/S0140-6736(74)91639-0
5. Teasdale G, Murray G, Parker L, Jennett B. Adding up the Glasgow Coma Score. *Acta Neurochir Suppl (Wien)*. 1979;28(1):13-16. doi:10.1007/978-3-7091-4088-8_2
6. Kay T, Harrington D, Adams R, et al. Definition of mild traumatic brain injury. *J Head Trauma Rehabil*. 1993.
7. Scholten AC, Haagsma JA, Panneman MJM, Van Beeck EF, Polinder S. Traumatic brain injury in the Netherlands: incidence, costs and disability-adjusted life years. *PLoS One*. 2014;9(10). doi:10.1371/JOURNAL.PONE.0110905
8. Kumar P, Clarck M. Traumatic brain injury. In: *Clinical Medicine*. 8th ed. Saunders Elsevier; 2012:1134.
9. Poirier MP. Concussions: assessment, management, and recommendations for return to activity. *Clin Pediatr Emerg Med*. 2003;4(3):179-185. doi:10.1016/S1522-8401(03)00061-2
10. Cancelliere C, Kristman VL, Cassidy JD, et al. Systematic Review of Return to Work After Mild Traumatic Brain Injury: Results of the International Collaboration on Mild Traumatic Brain Injury Prognosis. *Arch Phys Med Rehabil*. 2014;95(3):S201-S209. doi:10.1016/J.APMR.2013.10.010
11. van der Naalt J, Timmerman ME, de Koning ME, et al. Early predictors of outcome after mild traumatic brain injury (UPFRONT): an observational cohort study. *Lancet Neurol*. 2017;16(7):532-540. doi:10.1016/S1474-4422(17)30117-5
12. Wäljas M, Iverson GL, Lange RT, et al. A Prospective Biopsychosocial Study of the Persistent Post-Concussion Symptoms following Mild Traumatic Brain Injury. *J Neurotrauma*. 2015;32(8):534-547. doi:10.1089/NEU.2014.3339
13. Lingsma HF, Yue JK, Maas AIR, et al. Outcome Prediction after Mild and Complicated Mild Traumatic Brain Injury: External Validation of Existing Models and Identification of New Predictors Using the TRACK-TBI Pilot Study. *J Neurotrauma*. 2015;32(2):83-94. doi:10.1089/NEU.2014.3384
14. Laskowski RA, Creed JA, Raghupathi R. Pathophysiology of Mild TBI. In: Kobeissy FH, ed. *Brain Neurotrauma: Molecular, Neuropsychological, and Rehabilitation Aspects*. CRC Press/Taylor & Francis; 2015:35-42. doi:10.1201/b18126
15. Bazarian JJ, Blyth B, Mookerjee S, He H, McDermott MP. Sex Differences in Outcome after Mild Traumatic Brain Injury. *J Neurotrauma*. 2010;27(3):527. doi:10.1089/NEU.2009.1068
16. Niogi SN, Mukherjee P. Diffusion tensor imaging of mild traumatic brain injury. *J Head Trauma Rehabil*. 2010;25(4):241-255. doi:10.1097/HTR.0B013E3181E52C2A
17. Borg J, Holm L, Cassidy JD, et al. Diagnostic procedures in mild traumatic brain injury: results of the WHO Collaborating Centre Task Force on Mild Traumatic Brain Injury. *J Rehabil Med*. 2004;(43 Suppl):61-75. doi:10.1080/16501960410023822
18. Indicaties CT volwassenen met LTH - Richtlijn - Richtlijnendatabase. https://richtlijnendatabase.nl/richtlijn/licht_traumatisch_hoofd_hersenletsel_lth/indicaties_ct_volwassenen_met_lth.html. Accessed September 21, 2023.

19. Lewine JD, Davis JT, Bigler ED, et al. Objective documentation of traumatic brain injury subsequent to mild head trauma: multimodal brain imaging with MEG, SPECT, and MRI. *J Head Trauma Rehabil*. 2007;22(3):141-155. doi:10.1097/01.HTR.0000271115.29954.27

20. Belanger HG, Vanderploeg RD, Curtiss G, Warden DL. Recent neuroimaging techniques in mild traumatic brain injury. *J Neuropsychiatry Clin Neurosci*. 2007;19(1):5-20. doi:10.1176/jnp.2007.19.1.5

21. Stenberg J, Eikenes L, Moen KG, Vik A, Håberg AK, Skandsen T. Acute Diffusion Tensor and Kurtosis Imaging and Outcome following Mild Traumatic Brain Injury. *J Neurotrauma*. 2021;38(18):2560-2571. doi:10.1089/neu.2022.0206

22. Shahim P, Tegner Y, Marklund N, Blennow K, Zetterberg H. Neurofilament light and tau as blood biomarkers for sports-related concussion. *Neurology*. 2018;90(20):e1780-e1788. doi:10.1212/WNL.0000000000005518

23. Metting Z, Wilczak N, Rodiger LA, Schaaf JM, Van Der Naalt J. GFAP and S100B in the acute phase of mild traumatic brain injury. *Neurology*. 2012;78(18):1428-1433. doi:10.1212/WNL.0B013E318253D5C7

24. Vos PE, Lamers KJB, Hendriks JCM, et al. Glial and neuronal proteins in serum predict outcome after severe traumatic brain injury. *Neurology*. 2004;62(8):1303-1310. doi:10.1212/01.WNL.0000120550.00643.DC

25. Gardner RC, Rubenstein R, Wang KKW, et al. Age-Related Differences in Diagnostic Accuracy of Plasma Glial Fibrillary Acidic Protein and Tau for Identifying Acute Intracranial Trauma on Computed Tomography: A TRACK-TBI Study. *https://home.liebertpub.com/neu*. 2018;35(20):2341-2350. doi:10.1089/NEU.2018.5694

26. Bazarian JJ, Biberthaler P, Welch RD, et al. Serum GFAP and UCH-L1 for prediction of absence of intracranial injuries on head CT (ALERT-TBI): a multicentre observational study. *Lancet Neurol*. 2018;17(9):782-789. doi:10.1016/S1474-4422(18)30231-X

27. Gill J, Merchant-Borna K, Jeromin A, Livingston W, Bazarian J. Acute plasma tau relates to prolonged return to play after concussion. *Neurology*. 2017;88(6):595-602. doi:10.1212/WNL.0000000000003587

28. van der Horn HJ, Out ML, de Koning ME, et al. An integrated perspective linking physiological and psychological consequences of mild traumatic brain injury. *J Neurol*. 2020;267(9):2497. doi:10.1007/S00415-019-09335-8

29. Pasinetti GM, Fivecoat H, Ho L. Personalized Medicine in Traumatic Brain Injury. *Psychiatr Clin North Am*. 2010;33(4):905-913. doi:10.1016/J.PSC.2010.09.003

30. Arciniegas DB. Clinical electrophysiologic assessments and mild traumatic brain injury: State-of-the-science and implications for clinical practice. *Int J Psychophysiol*. 2011;82(1):41-52. doi:10.1016/J.IJPSYCHO.2011.03.004

31. Tewarie PKB, Beernink TMJ, Eertman-Meyer CJ, et al. Early EEG monitoring predicts clinical outcome in patients with moderate to severe traumatic brain injury. *NeuroImage Clin*. 2023;37:103350. doi:10.1016/J.NICL.2023.103350

32. Van Putten MJAM, Peters JM, Mulder SM, De Haas JAM, Bruijninckx CMA, Tavy DLJ. A brain symmetry index (BSI) for online EEG monitoring in carotid endarterectomy. *Clin Neurophysiol*. 2004;115(5):1189-1194. doi:10.1016/J.CLINPH.2003.12.002

33. Vespa PM, Boscardin WJ, Hovda DA, et al. Early and persistent impaired percent alpha variability on continuous electroencephalography monitoring as predictive of poor outcome after traumatic brain injury. *J Neurosurg*. 2002;97(1):84-92. doi:10.3171/JNS.2002.97.1.0084

34. Korn A, Golan H, Melamed I, Pascual-Marqui R, Friedman A. Focal cortical dysfunction and blood-brain barrier disruption in patients with postconcussion syndrome. *J Clin Neurophysiol*. 2005;22(1):1-9. doi:10.1097/01.WNP.0000150973.24324.A7

35. Chen X-P, Tao L-Y, Chen ACN. Electroencephalogram and evoked potential parameters examined in Chinese mild head injury patients for forensic medicine. *Neurosci Bull*. 2006;22(3):165-170.

36. Montgomery EA, Fenton GW, McClelland RJ, MacFlynn G, Rutherford WH. The psychobiology of minor head injury. *Psychol Med*. 1991;21(2):375-384. doi:10.1017/S0033291700020481

37. Thatcher RW, Cantor DS, McAlaster R, Geisler F, Krause P. Comprehensive Predictions of Outcome in Closed Head-Injured Patients. *Ann N Y Acad Sci*. 1991;620(1):82-101. doi:10.1111/J.1749-6632.1991.TB51576.X

38. Thatcher RW, North DM, Curtin RT, et al. An EEG severity index of traumatic brain injury. *J Neuropsychiatry Clin Neurosci*. 2001;13(1):77-87. doi:10.1176/JNP.13.1.77

39. Thatcher RW, Walker RA, Gerson I, Geisler FH. EEG discriminant analyses of mild head trauma. *Electroencephalogr Clin Neurophysiol*. 1989;73(2):94-106. doi:10.1016/0013-4694(89)90188-0

40. Williams BR, Lazic SE, Ogilvie RD. Polysomnographic and quantitative EEG analysis of subjects with long-term insomnia complaints associated with mild traumatic brain injury. *Clin Neurophysiol*. 2008;119(2):429-438. doi:10.1016/J.CLINPH.2007.11.003

41. Hessen E, Nestvold K. Indicators of complicated mild TBI predict MMPI-2 scores after 23 years. *Brain Inj*. 2009;23(3):234-242. doi:10.1080/02699050902748349

42. Denker PG, Perry GF. Postconcussion Syndrome in Compensation and Litigation; Analysis of 95 Cases with Electroencephalographic Correlations. *Neurology*. 1954;4(12):912-912. doi:10.1212/WNL.4.12.912

43. Koufen H, Dichgans J. Frequency and course of posttraumatic EEG-abnormalities and their correlations with clinical symptoms: a systematic follow up study in 344 adults (author's transl). *Fortschr Neurol Psychiatr Grenzgeb*. 1978;46(4):165-177.

44. Torres F, Shapiro SK. Electroencephalograms in whiplash injury. A comparison of electroencephalographic abnormalities with those present in closed head injuries. *Arch Neurol*. 1961;5(1):28-35. doi:10.1001/ARCHNEUR.1961.00450130030005

45. Voller B, Benke T, Benedetto K, Schnider P, Auff E, Aichner F. Neuropsychological, MRI and EEG findings after very mild traumatic brain injury. *Brain Inj*. 1999;13(10):821-827. doi:10.1080/026990599121214

46. Jacome DE. EEG in whiplash: a reappraisal. *Clin Electroencephalogr*. 1987;18(1):41-45.

47. Nuwer MR, Hovda DA, Schrader LM, Vespa PM. Routine and quantitative EEG in mild traumatic brain injury. *Clin Neurophysiol*. 2005;116(9):2001-2025. doi:10.1016/J.CLINPH.2005.05.008

48. de Koning ME, Gareb B, El Moumni M, et al. Subacute posttraumatic complaints and psychological distress in trauma patients with or without mild traumatic brain injury. *Injury*. 2016;47(9):2041-2047. doi:10.1016/J.INJURY.2016.04.036

49. van der Naalt J, van Zomeren AH, Sluiter WJ, Minderhoud JM. One year outcome in mild to moderate head injury: the predictive value of acute injury characteristics related to complaints and return to work. *J Neurol Neurosurg Psychiatry*. 1999;66(2):207-213. doi:10.1136/JNNP.66.2.207

50. Wilson L, Boase K, Nelson LD, et al. A Manual for the Glasgow Outcome Scale-Extended Interview. *J Neurotrauma*. 2021;38(17):2435-2446. doi:10.1089/neu.2020.7527

51. Berger H. Über das Elektrenkephalogramm des Menschen. *Arch Psychiatr Nervenkr*. 1929;87(1):527-570. doi:10.1007/BF01797193/METRICS

52. Sreeja SR, Rajmohan S, Sodhi MS, Samanta D, Mitra P. Dictionary Learning and Greedy Algorithms for Removing Eye Blink Artifacts from EEG Signals. *Circuits, Syst Signal Process*. 2023;42(9):5663-5683. doi:10.1007/S00034-023-02381-8/FIGURES/10

53. Tatum WO. Ellen R. Grass Lecture: Extraordinary EEG. *Neurodiagn J*. 2014;54(1):3-21. doi:10.1080/21646821.2014.11079932

54. De Koning ME, Scheenen ME, Van Der Horn HJ, Spikman JM, Van Der Naalt J. From 'miserable minority' to the 'fortunate few': the other end of the mild traumatic brain injury spectrum. *Brain Inj*. 2018;32(5):540-543. doi:10.1080/02699052.2018.1431844

55. Miller NR, Yasen AL, Maynard LF, Chou LS, Howell DR, Christie AD. Acute and longitudinal changes in motor cortex function following mild traumatic brain injury. *Brain Inj*. 2014;28(10):1270-1276. doi:10.3109/02699052.2014.915987

56. Kaltiainen H, Helle L, Liljeström M, Renvall H, Forss N. Theta-Band Oscillations as an Indicator of Mild Traumatic Brain Injury. *Brain Topogr*. 2018;31(6):1037. doi:10.1007/S10548-018-0667-2

57. Steriade M, Gloor P, Llinás RR, Lopes da Silva FH, Mesulam MM. Report of IFCN Committee on Basic Mechanisms. Basic mechanisms of cerebral rhythmic activities. *Electroencephalogr Clin Neurophysiol*. 1990;76(6):481-508. doi:10.1016/0013-4694(90)90001-Z

58. Thatcher RW, Biver C, McAlaster R, Salazar A. Biophysical linkage between MRI and EEG coherence in closed head injury. *Neuroimage*. 1998;8(4):307-326. doi:10.1006/NIMG.1998.0365

59. Lewine JD, Plis S, Ulloa A, et al. Quantitative EEG Biomarkers for Mild Traumatic Brain Injury. *J Clin Neurophysiol*. 2019;36(4):298-305. doi:10.1097/WNP.0000000000000588

60. Marzolla MC, Wijenberg M, Stapert S, Hurks P, Schepers J, Van Heugten C. Hypersensitivity to Noise and Light over 1 Year after Mild Traumatic Brain Injury: A Longitudinal Study on Self-Reported Hypersensitivity and Its Influence on Long-Term Anxiety, Depression, and Quality of Life. *J Head Trauma Rehabil*. 2023;38(3):259-267. doi:10.1097/HTR.0000000000000813

61. Hoek AE, Geraerds AJLM, Rood PPM, et al. The Effect of Written and Video Discharge Instructions after Mild Traumatic Brain Injury on Healthcare Costs and Productivity Costs. *J Head Trauma Rehabil*. 2022;37(4):E231-E241. doi:10.1097/HTR.0000000000000720

62. Bossers SM, Pol KM, Oude Ophuis EPA, et al. Discrepancy between the initial assessment of injury severity and post hoc determination of injury severity in patients with apparently mild traumatic brain injury: a retrospective multicenter cohort analysis. *Eur J Trauma Emerg Surg*. 2018;44(6):889-896. doi:10.1007/S00068-017-0861-Z/TABLES/3

63. Wilson JTL, Pettigrew LEL, Teasdale GM. Structured interviews for the Glasgow Outcome Scale and the extended Glasgow Outcome Scale: guidelines for their use. *J Neurotrauma*. 1998;15(8):573-580. doi:10.1089/NEU.1998.15.573

64. Levin HS, Boake C, Song J, et al. Validity and sensitivity to change of the extended Glasgow Outcome Scale in mild to moderate traumatic brain injury. *J Neurotrauma*. 2001;18(6):575-584. doi:10.1089/089771501750291819

65. Rabinowitz AR, Levin HS. Cognitive Sequelae of Traumatic Brain Injury. *Psychiatr Clin North Am*. 2014;37(1):1. doi:10.1016/J.PSC.2013.11.004

66. Iverson GL, Lange RT, Brooks BL, Rennison VLA. "Good Old Days" Bias Following Mild Traumatic Brain Injury. *Clin Neuropsychol*. 2010;24(1):17-37. doi:10.1080/13854040903190797

67. Sheorajpanday RVA, Nagels G, Weeren AJTM, van Putten MJAM, De Deyn PP. Reproducibility and clinical relevance of quantitative EEG parameters in cerebral ischemia: a basic approach. *Clin Neurophysiol*. 2009;120(5):845-855. doi:10.1016/J.CLINPH.2009.02.171

68. Cheng Q, Yang W, Liu K, et al. Increased Sample Entropy in EEGs During the Functional Rehabilitation of an Injured Brain. *Entropy 2019, Vol 21, Page 698*. 2019;21(7):698. doi:10.3390/E21070698

69. Haveman ME, Van Putten MJAM, Hom HW, Eertman-Meyer CJ, Beishuizen A, Tjepkema-Cloostermans MC. Predicting outcome in patients with moderate to severe traumatic brain injury using electroencephalography. *Crit Care*. 2019;23(1):1-9. doi:10.1186/S13054-019-2656-6/FIGURES/3

70. Wang J, Huang L, Ma X, Zhao C, Liu J, Xu D. Role of Quantitative EEG and EEG Reactivity in Traumatic Brain Injury. *Clin EEG Neurosci*. 2022;53(5):452-459. doi:10.1177/1550059420984934

Appendix 1 – Questionnaires

Head Injury Symptom Checklist

Wilt u aangeven of u last had/hebt van één of meer van de volgende klachten? Kruis steeds in de eerste kolom de situatie voor het ongeval en in de tweede kolom de klachten op dit moment

	Voor het ongeval			Heden, na het ongeval		
	Nee	Soms	Vaak	Nee	Soms	Vaak
Hebt u last van hoofdpijn?	O	O	O	O	O	O
Bent u duizelig of licht in het hoofd?	O	O	O	O	O	O
Hebt u last van evenwichtsstoornissen?	O	O	O	O	O	O
Hebt u last van oorsuizen?	O	O	O	O	O	O
Hebt u last van gehoorsverlies?	O	O	O	O	O	O
Hebt u veel slaap nodig?	O	O	O	O	O	O
Wordt u snel moe?	O	O	O	O	O	O
Bent u vergeetachtig?	O	O	O	O	O	O
Hebt u moeite zich te concentreren?	O	O	O	O	O	O
Bent u traag?	O	O	O	O	O	O
Bent u prikkelbaar, snel kwaad?	O	O	O	O	O	O
Kunt u slecht tegen lawaai?	O	O	O	O	O	O
Kunt u slecht tegen alcohol?	O	O	O	O	O	O
Bent u angstig of hebt u angstige dromen?	O	O	O	O	O	O
Hebt u last van een droge mond?	O	O	O	O	O	O
Hebt u pijn in de nek?	O	O	O	O	O	O
Hebt u een stijve nek?	O	O	O	O	O	O
Hebt u pijn in de armen?	O	O	O	O	O	O
Hebt u last van jeuk?	O	O	O	O	O	O

Glasgow Outcome Scale – Extended

Deze vragen gaan over het functioneren in het dagelijkse leven.

1 Bent u in staat om te spreken of eenvoudige opdrachten uit te voeren?

- ☐ Nee
- ☐ Ja

2a Heeft u hulp nodig bij bepaalde dagelijkse activiteiten?
(*wassen, aankleden, eten, eten klaarmaken)*

- ☐ Nee ► Ga naar vraag 3
- ☐ Ja

2b Hoe vaak heeft u hulp nodig?

- ☐ 24 uur per dag
- ☐ Kan tot 8 uur per dag alleen zijn

2c Was u voor het ongeval thuis onafhankelijk? ☐ Ja ☐ Nee

3a Kunt u zonder hulp boodschappen doen? ☐ Ja ☐ Nee

3b Kon u dit voor het ongeval? ☐ Ja ☐ Nee

4a Kunt u zich zonder hulp in de buurt verplaatsen? ☐ Ja ☐ Nee

4b Kon u dit voor het ongeval? ☐ Ja ☐ Nee

5a Bent u momenteel in staat te werken/naar school te gaan of voor anderen to zorgen op uw oude niveau?

- ☐ Ja, volledig ► Ga naar vraag 6
- ☐ Nee, of slechts gedeeltelijk

5b. Wat is de mate van arbeidsongeschiktheid?

- ☐ Gedeeltelijk
- ☐ Volledig, aangepast of ander werk dan voorheen

5c. Werkte u voor het ongeval of was u werkzoekend?

- ☐ Ja
- ☐ Nee

6a Heeft u uw reguliere sociale contacten en vrijetijdsbestedingen buitenshuis weer volledig hervat?

- ☐ Ja ► Ga naar vraag 7
- ☐ Nee

6b In hoeverre wordt u beperkt in de omgang met anderen en in uw vrijetijdsbesteding?

- ☐ Ik ben minder actief, maar ten minste op 50% van mijn oude niveau
- ☐ Ik ben veel minder actief, minder dan 50% dan voor het ongeval
- ☐ Ik doe nog maar zelfden of nooit wat buitenshuis

6c Had u voor het ongeval regelmatig omgang met anderen en vrijetijdsbesteding buitenshuis?

- ☐ Ja
- ☐ Nee

7a Is er bij u sprake van psychische problemen waardoor er problemen ontstaan zijn binnen het gezin, de familie of de vriendenkring (*Bijvoorbeeld: opvliegendheid, prikkelbaarheid, irritaties, angsten, wisselend humeur, onredelijkheid of depressies)*

- ☐ Ja
- ☐ Nee ► Ga naar vraag 8

7b Hoe vaak treden deze problemen op?

- ☐ Soms: minder dan wekelijks
- ☐ Vaak: een keer per week of vaker, maar acceptabel
- ☐ Constant: dagelijks en onverdraaglijk

7c Als deze problemen anders dan voor het ongeval?

- ☐ Ja
- ☐ Nee
- ☐ N.v.t.

8a Zijn er op dit moment andere klachten ten gevolge van het ongeval die **van invloed** zijn op het dagelijkse leven? (*Bijvoorbeeld: hoofdpijn, duizeligheid, moeheid, geheugen- en concentratiestoornissen)*

- ☐ Ja
- ☐ Nee

8b Als deze klachten al voor het ongeval bestonden, zijn ze dan erger geworden?

- ☐ Ja
- ☐ Nee
- ☐ N.v.t.

8c Wat is voor u de belangrijkste veroorzaker van alle gevolgen na het ongeval?

- ☐ Het hoofd- en/of hersenletsel
- ☐ Letsel aan andere lichaamsdelen
- ☐ Een combinatie

Appendix 2 – Explanation on number of datasets

For this research we used four signal analyses approaches (relative power, power variability, power symmetry and coherence). Per approach, many different situations could be distinguished, based on variables such as eye state (open and closed), phase (acute, subacute and differences in between the phases), frequency bands (theta, alpha and beta) and lead-signals (19) or lead-signal-pairs (up to 58). The number of variables differs per approach. All different situations of all four approaches combined come down to 909. This means that 909 datasets could be compared to both HISC scores and GOS-E outcomes. See Table 12 and Figure 12A for an explanation on this number. This high number would potentially jeopardise the significance of the statistical analyses in this study. Therefore, we had to reduce the amount of statistical analyses, and thus the amount of datasets had to be reduced. After applying the divergence-selection-algorithm, the number of datasets was reduced to 78. See Table 13 and Figure 12B for an explanation on this reduction.

Table 12. Explanation on the amount of data-sets generated by the signal analyses (all four approaches). Note that the numbers in each row are multiplied to get to the amount in the 'Total' column. We had to reduce the amount of datasets to limit the influence on the significance of the statistical tests that had yet to be performed. [1]The acute phase, subacute phase and the difference between acute and subacute as the third 'phase'.

Approach	Phases[1]	Frequency bands	Eye states	Leads/lead-pairs	Total
Relative power	3	3	2	19	342
Power variability	3	3	1	19	171
Power symmetry	3	1	2	8	48
Coherence	3	1	2	58	348
Total number of possible datasets					909

Table 13. Explanation on the amount of datasets generated after the divergence-selection-algorithm (all four approaches). Note that the numbers in each row are multiplied to get to the amount in the 'Total' column. This also represents the amount of datasets that we statistically analysed. [1]The acute phase, subacute phase and the difference between acute and subacute as the third 'phase'.

Approach	Phases[1]	Frequency bands	Eye states	Divergent leads/ lead-pairs	Total
Relative power	3	3	2	2	36
Power variability	3	3	1	2	18
Power symmetry	3	1	2	2	12
Coherence	3	1	2	2	12
Total number of possible datasets					78

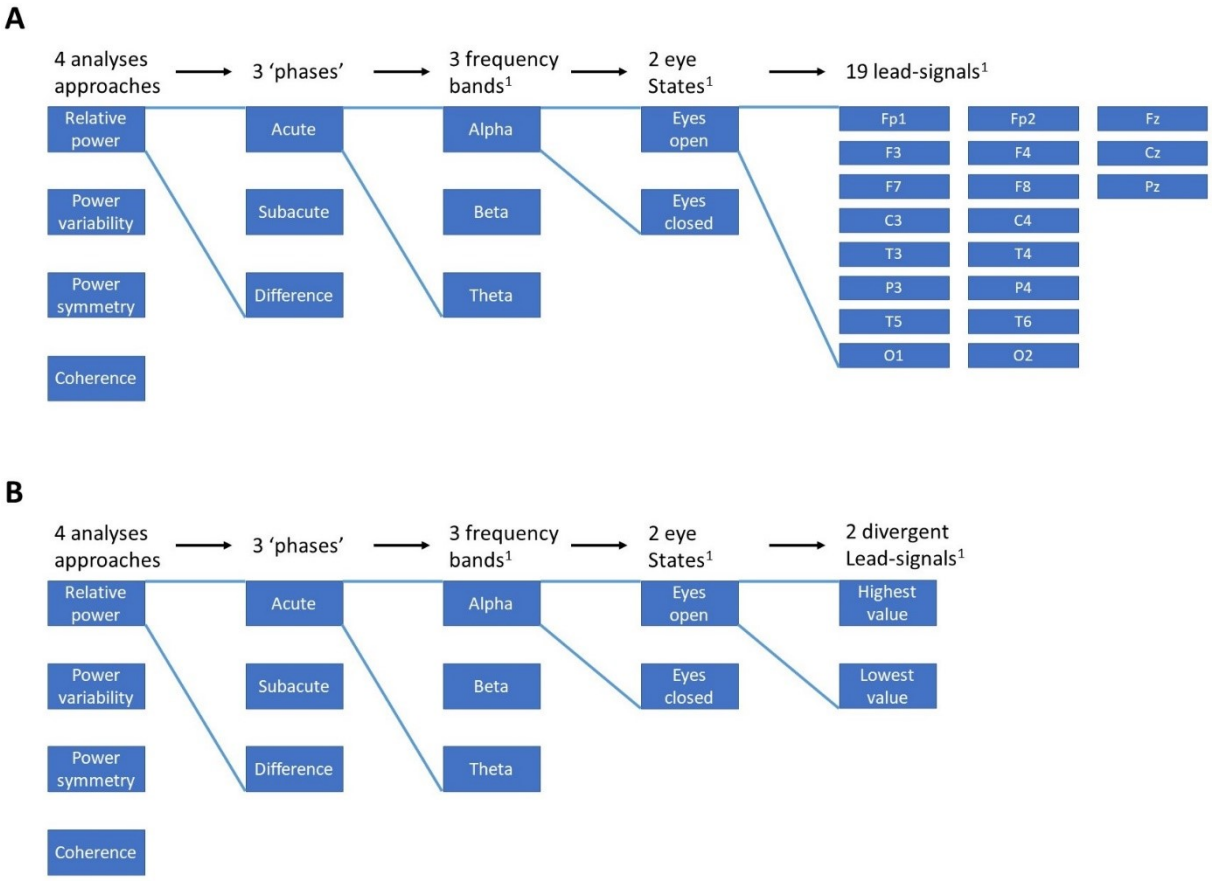

Figure 12. A. Explanation on the amount of datasets generated by the signal analyses. One of four approaches, relative power, is taken as an example. In this approach, we had to analyse two phases and the differences in between these phases. Per phase, three frequency bands had to be analysed. Per band there are two eye states we analysed and per eye state are 19 lead-signals we could have analysed. B. Explanation on the amount after reduction by the divergence-selection-algorithm. Instead of generating a dataset for all lead-signals or lead-signal-pairs given every situation, two datasets are created given every situation. [1]In case of the relative power signal analysis approach; numbers differ in other approaches.

Appendix 3 – Validation of the divergence-selection-algorithm

We validated the divergence-selection-algorithm in all four approaches using simulations. A virtual brain was simulated for every approach with a given amount of simulated lead-signals. Three lead-signals represented a 'healthy' signal, at least one 'unhealthy' lead produced a signal that should in theory give a low score after signal analysis and one 'unhealthy' lead that should give a high score. We also created two 'decoy signals' that should also score lower and higher than the 'healthy signals', but not as low and high as the previously mentioned unhealthy signals. Given the signal analyses approaches work well, they should be able to pick out the low and high scoring lead-signals and not the decoy or healthy signals. To acquire healthy population data we created an additional set of ten healthy signals. Since all lead-signals in the 'virtual brain' have at default (in 'healthy state') similar properties, one set of healthy signals is sufficient to determine healthy population averages for the signal analysis results at all leads of the virtual brain. Per signal analyses approach, the above described simulation was repeated 1,000 times.

The signals $Signal_{sim}$ generated for the validation of the relative power, power variability and power symmetry approaches are a summation of a random signal and three sets of sinusoids:

$$Signal_{sim} = Signal_{rand} + A_{set\,1} \sum Sinusoids_{set\,1} + A_{set\,2} \sum Sinusoids_{set\,2} + A_{set\,3} \sum Sinusoids_{set\,3} \quad (5)$$

$Signal_{rand}$ is a signal with pseudorandom values within the interval -100 – +100 µV and has a uniform distribution. Amplitudes $A_{set\,n}$ are at default set at 3 µV. The sets of sinusoids are stored in a matrix and defined as:

$$Sinusoids_{set\,n} = \sin(f_n * 2\pi * t * \tau) \quad (6)$$

Time variation τ is defined as:

$$\tau = [0.9 : 0.01 : 1.1] \quad (7)$$

We chose three base frequencies f_n at 6, 10 and 20 Hz. These frequencies correspond to the theta, alpha and beta bands respectively while also complying to the 1 – 25 Hz range of the power symmetry analyses. See Figure 13 for a typical power spectral density estimate plot of $Signal_{sim}$.

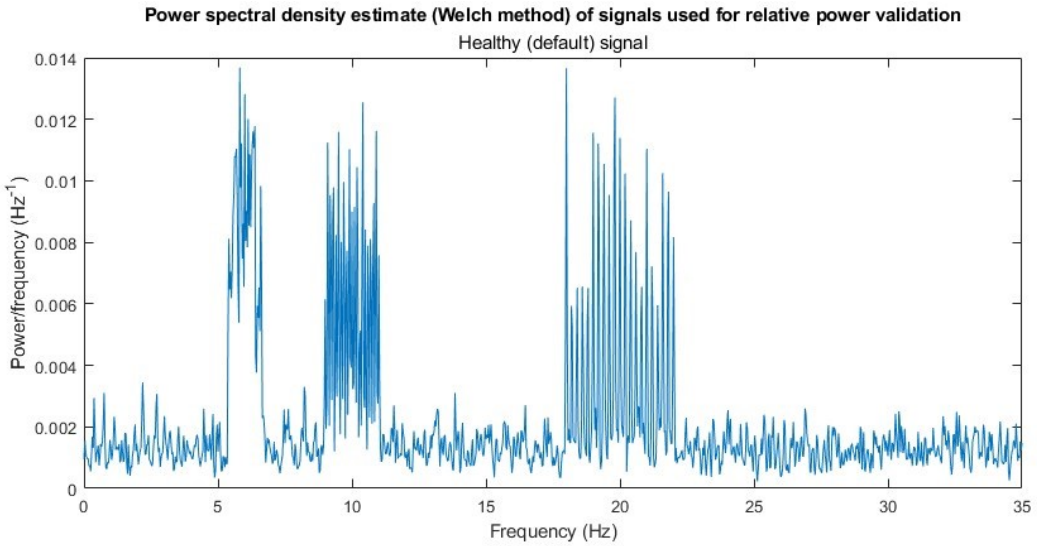

Figure 13. Power spectral density estimate of a 'healthy' signal used to validate the divergence-selection-algorithm within the relative power approach. Note the increased power around the three sets of sinusoids (around 6, 10 and 20 Hz).

To generate the 'unhealthy' signals, we adjusted the amplitudes. The default length of the signals was 2 minutes with a sample frequency of 512 Hz. For a full overview of all generated signals per analyses approach, see Tables 14 – 17.

Relative power

To test the divergence-selection-algorithm in the relative power approach, we created ten 'healthy' signals, having default amplitudes, as well as ten test signals. Of these test signals, three were 'healthy' signals. To test the ability to pick out divergent signals at the theta band, one 'target' signal had an amplitude half that of the healthy signals of the 6 Hz sinusoids and one 'target' signal had a double amplitude at the same sinusoids. These signals ought to be picked out by the divergence-selection-algorithm as the most divergent (low and high scoring) signals when analysing the theta band. To test the same principle at the alpha and beta band, similar target signals were created with adjusted amplitudes at the 10 and 20 Hz sinusoids. Two 'decoy' signals were created by one having all its sinusoid amplitudes being 0.75 times that of the default amplitude and one having sinusoid amplitudes of 1.5 times default. These signals should score more divergent than the healthy signals, yet not as divergent as the target signals and therefore ought not to be picked out by the selection-algorithm. For an overview of the signals we created to validate the relative power approach, see Table 14.

Table 14. Overview of signals created to validate the divergence-selection-algorithm in the relative power approach.

Signal label	Random signal amplitude (µV)	+ 6 Hz sinusoids amplitude (µV)	+ 10 Hz sinusoids amplitude (µV)	+ 20 Hz sinusoids amplitude (µV)
	10 healthy signals			
Healthy	100	1	3	3
	Test signals			
Healthy	100	3	3	3
Healthy	100	3	3	3
Healthy	100	3	3	3
Theta low	100	1.5	3	3
Theta high	100	6	3	3
Alpha low	100	3	1.5	3
Alpha high	100	3	6	3
Beta low	100	3	3	1.5
Beta high	100	3	3	6
Decoy low	100	3.75	3.75	3.75
Decoy high	100	5.25	5.25	5.25

Power variability

To validate the divergence-selection-algorithm in the power variability approach, we used ten healthy signals and ten test signals. We created these signals by joining together two two-minute long signals with different amplitudes. Due to the differences in amplitude, the new created signals have a predictable level of variability. The first half of healthy signals has amplitudes of 3 µV (default) and the second half has amplitudes of 4.5 µV (1.5 times default). The set of test signals had three signals similar to the healthy signals. The test signal that should yield the highest variability in the alpha band has set the alpha amplitudes to 6 µV (2 times default) and the signal that should yield the lowest alpha band variability has set these same amplitudes to 3 µV (1 times default). In a similar way we created two signals that should yield the lowest and highest variability in the beta band and two signals in the theta band. Additionally, we created two 'decoy' signals; one had all its amplitudes set to 3.75 µV (1.25 times default) and one to 5.25 µV (1.75 times default). The divergence-selection-algorithm should not pick out these decoy signals. For an overview of the created signals we used to validate the power variability approach, see Table 15.

Power symmetry

To test the divergence-selection-algorithm in the power symmetry approach, we performed a similar simulation. In this case, we did create and analyse not individual signals, but sets of signals. To gain the healthy population average, we created ten sets; ten signals as earlier described with default (3 µV) amplitudes were compared to signals with amplitudes of 4.5 µV (1.5 times default). We created seven test signal sets of which three sets were similar to the healthy sets (1 versus 1.5 times default amplitude). The remaining sets were comparable, although we adjusted the amplitudes of the 10 Hz sinusoids. In one set, the amplitude of the 10 Hz sinusoids is set to default (3 µV). This set should score the best symmetry score and therefore ought to be picked out by the algorithm. In another set, we set this amplitude to 2 times default and therefore this set should score lower in the symmetry calculations and ought to be picked out as well. The two final sets were decoys with intermediate amplitudes at 1.25 and 1.75 times default amplitude. For an overview of the created signals used to validate the power symmetry approach, see Table 16.

Table 15. Overview of signals created to validate the divergence-selection-algorithm in the power variability approach.

Signal label	Random signal amplitude (µV)	+ 6 Hz sinusoids amplitude (µV)	+ 10 Hz sinusoids amplitude (µV)	+ 20 Hz sinusoids amplitude (µV)		Random signal amplitude (µV)	+ 6 Hz sinusoids amplitude (µV)	+ 10 Hz sinusoids amplitude (µV)	+ 20 Hz sinusoids amplitude (µV)
	10 healthy signals								
Healthy	100	3	3	3	followed by	100	4.5	4.5	4.5
	Test signals								
Healthy	100	3	3	3	followed by	100	4.5	4.5	4.5
Healthy	100	3	3	3		100	4.5	4.5	4.5
Healthy	100	3	3	3		100	4.5	4.5	4.5
Theta low	100	3	3	3		100	3	4.5	4.5
Theta high	100	3	3	3		100	6	4.5	4.5
Alpha low	100	3	3	3		100	4.5	3	4.5
Alpha high	100	3	3	3		100	4.5	6	4.5
Beta low	100	3	3	3		100	4.5	4.5	3
Beta high	100	3	3	3		100	4.5	4.5	6
Decoy low	100	3	3	3		100	3.75	3.75	3.75
Decoy high	100	3	3	3		100	5.25	5.25	5.25

Table 16. Overview of signals created to validate the divergence-selection-algorithm in the power symmetry approach.

Signal label	Random range amplitude (µV)	+ 6 Hz sinusoids amplitude (µV)	+ 10 Hz sinusoids amplitude (µV)	+ 20 Hz sinusoids amplitude (µV)		Random range amplitude (µV)	+ 6 Hz sinusoids amplitude (µV)	+ 10 Hz sinusoids amplitude (µV)	+ 20 Hz sinusoids amplitude (µV)
	10 healthy signals								
Healthy	100	3	3	3	Compared to	100	4.5	4.5	4.5
	Test signals								
Healthy	100	3	3	3	Compared to	100	4.5	4.5	4.5
Healthy	100	3	3	3		100	4.5	4.5	4.5
Healthy	100	3	3	3		100	4.5	4.5	4.5
Low	100	3	3	3		100	4.5	6	4.5
High	100	3	3	3		100	4.5	3	4.5
Decoy low	100	3	3	3		100	4.5	5.25	4.5
Decoy high	100	3	3	3		100	4.5	3.75	4.5

Coherence

To test the coherence approach, we created signals in another way. Signals created in a way similar to these used in the other approach validations were not useful for validating coherence due to having a random signal as base signal. Two signals with a random signal as base score high on coherence, more or less regardless of additional sinusoids. Therefore, we created signals using a section of EEG-data from one of the patients. We visually inspected that section for the presence of artefacts and undesired waves, so that a clean 'neutral' section of EEG was used.

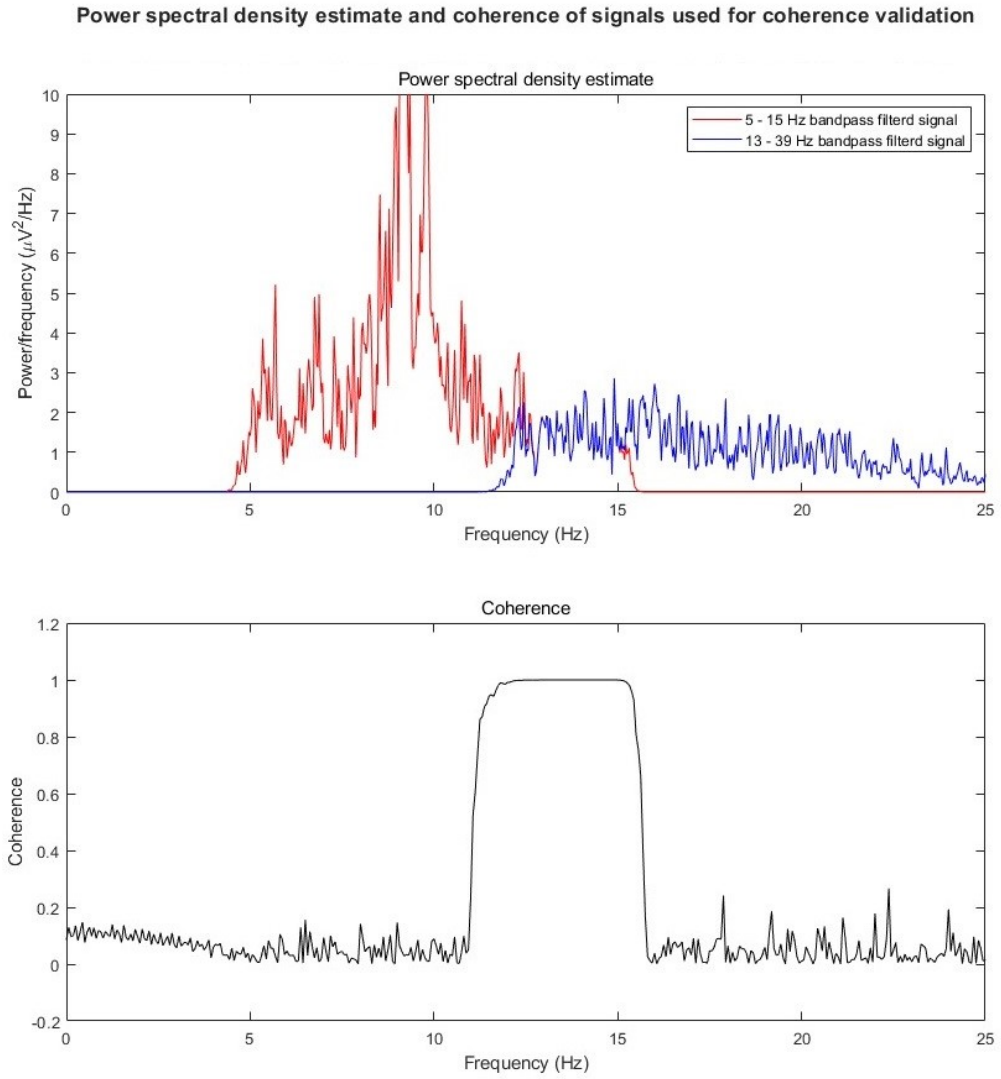

Figure 14. Power spectral density estimate (Welch's method) and coherence plot of two signals we used to validate the divergence-selection-algorithm within the coherence approach. This combination of signals should score relative low on coherence, considering the limited overlap in common frequencies. Another combination of signals has even less overlap, scoring an even lower coherence. Therefore, the combination depicted in this figure should not be picked out by the divergence-selection-algorithm and is therefore labelled as a 'decoy' combination.

We created signal-pairs to test the coherence approach, with each pair having the same base signal. This base signal is a rearranged version of the previously mentioned EEG-data section. The EEG-data section was cut at a random point and the two new sections were swapped. After the creation of the base signal, we bandpass filtered this signal twice to create the two signals which, in combination can be used to perform coherence calculations. The cutoff frequencies of the bandpass filters of the two signals overlap to a certain degree, depending on the desired level of coherence. See Figure 14 for a power spectral density estimate of such a signal-pair, displaying the overlap in frequencies.

For the ten healthy signal combinations, one signal was created using a 5 – 15 Hz bandpass filter (which is considered the default bandwidth), the other was created via a 10 – 30 Hz bandpass filter, having a 5 Hz range overlap. We created three test signal combinations using similar filters. The combination that should have the lowest coherence score had the second bandpass filter set at 14 – 42 Hz (1 Hz overlap). The combination with the highest coherence score had this filter set at 6 – 18 Hz (9 Hz overlap). The two decoy combinations we created had the filter set at 13 – 39 Hz (2 Hz overlap) and 7 – 21 Hz (8 Hz overlap). For an overview of all signals created to validate the coherence approach, see Table 17.

Table 17. Overview of signals created to validate the divergence-selection-algorithm in the coherence approach.

Signal label	Low cut-off frequency (Hz)	High cut-off frequency (Hz)		Low cut-off frequency (Hz)	High cut-off frequency (Hz)
			10 healthy signals		
Healthy	5	15	Compared to	10	30
			Test signals		
Healthy	5	15	Compared to	10	30
Healthy	5	15		10	30
Healthy	5	15		10	30
Low	5	15		14	42
High	5	15		6	18
Decoy low	5	15		13	39
Decoy high	5	15		7	21

Validation results

In all four signal analysis approaches, the validation of the divergence-selection-algorithm resulted in a success rate of 100%, e.g. all validation attempts were successful, given the methods of validation and the settings as described above.

Table 18. Succes rate results of the validation of the divergence-selection-algorithm.

Approach	Success rate (%)
Relative power	100.0
Power variability	100.0
Power symmetry	100.0
Coherence	99.9

Appendix 4 – Example of relative power approach process

First step in calculating the relative power scores is to select an EEG epoch. In this example, we used an eyes closed epoch in an EEG recording on a patient in the acute phase, specifically recorded at the Fp1 lead.

After selecting the EEG epoch, a power spectral density estimate (PSD) is calculated (see Figure 15). Within the PSD, the area under the curve is calculated, corresponding to the total bandwidth of the three used frequency bands, i.e. 3.5 – 30 Hz (lower graph). In a same manner, the area under the curve is calculated for the individual frequency bands. The upper graph, displays the area corresponding to the alpha band (8 – 13 Hz). In this example the power of the alpha frequency band is 100 μV^2 while the power corresponding to all frequency bands is 141 μV^2. Dividing these powers results in the relative power of 0.71. The relative power of the second eyes closed epoch in this particular EEG measurement is 0.72. The average of these relative powers is 0.71, which is stored as the closed eye score in this particular setting and patient (see Table 19 second column, bottom row and Tabel 20**Fout! Verwijzingsbron niet gevonden.** third column, bottom row).

Example of power spectral density estimate used in the relative power approach

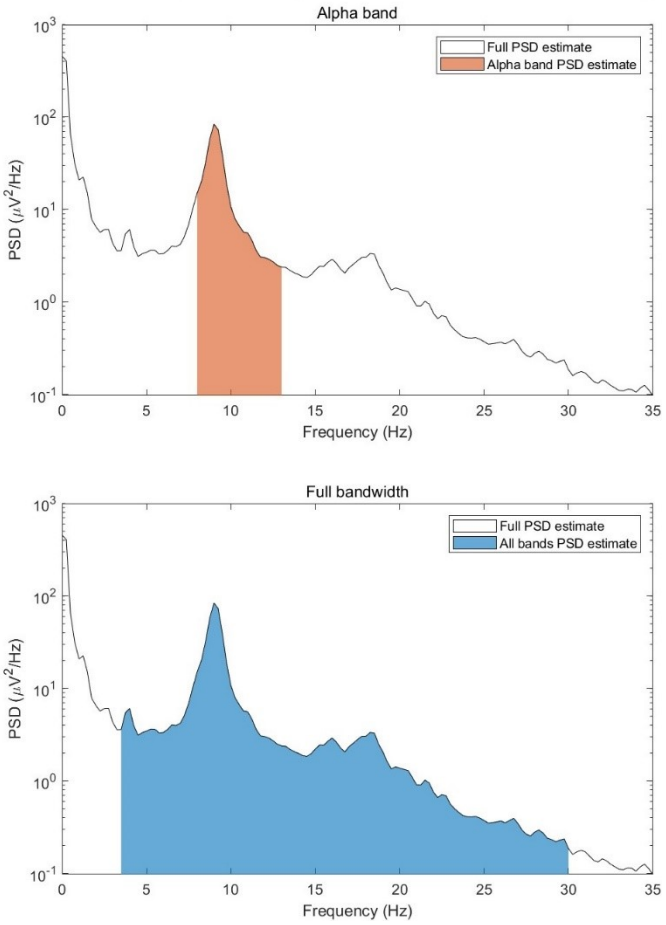

Figure 15. Power spectral density estimate used in one of the relative power approach calculations. The upper graph displays the area under the curve representing the alpha band (8 – 13 Hz). The lower graph represents the full bandwidth (theta, alpha and beta band combined, 3.5 – 30 Hz)

This process was repeated for all patients and control group subjects, for all frequency bands, leads, eye states (open/closed) and phases. The healthy group value corresponding to the example above (acute phase, alpha band, eyes closed, O2-lead) is 0.10. Therefore, the relative result in case of the patient in the previous example is 0.75 (see Equation 4 and see bottom row in Table 19).

The final step of the divergence-selection algorithm is selecting the highest and lowest relative scores. Table 19 displays the relative scores at all leads of the same patient and setting (alpha band, eyes closed) as in the example. The highest acute phase score is the O2 score (0.75) and the lowest is the T4 score (0.29). The O2 and T4 scores also happen to be the highest and lowest scores in the subacute phase (see Table 19).

Table 19. Example of the divergence-selection-algorithm processing of acute and subacute phase data. This table represents data from one patient. The relative scores (fourth and seventh column) are calculated using the original scores (second and fifth column) and the healthy population averages (third/sixth column). See Equation 4 for the relative score calculation. Per patient, the highest and lowest scoring leads are selected (green and red respectively).

Lead	Scores acute phase	Healthy population averages	Relative scores acute phase	Scores subacute phase	Healthy population averages	Relative scores subacute phase
Fp1	0.44	0.14	0.50	0.52	0.14	0.57
Fp2	0.43	0.16	0.47	0.50	0.16	0.52
F7	0.42	0.15	0.49	0.49	0.15	0.54
F3	0.45	0.15	0.50	0.55	0.15	0.57
Fz	0.47	0.14	0.54	0.56	0.14	0.60
F4	0.49	0.16	0.51	0.53	0.16	0.54
F8	0.41	0.16	0.45	0.47	0.16	0.50
T3	0.37	0.17	0.36	0.43	0.17	0.43
C3	0.37	0.19	0.33	0.50	0.19	0.45
Cz	0.49	0.18	0.47	0.54	0.18	0.51
C4	0.44	0.19	0.41	0.49	0.19	0.45
T4	0.33	0.18	0.29	0.40	0.18	0.38
T5	0.53	0.13	0.59	0.52	0.13	0.59
P3	0.44	0.15	0.49	0.46	0.15	0.51
Pz	0.41	0.15	0.46	0.45	0.15	0.51
P4	0.48	0.14	0.54	0.54	0.14	0.58
T6	0.55	0.12	0.63	0.67	0.12	0.69
O1	0.70	0.11	0.74	0.67	0.11	0.73
O2	0.71	0.10	0.75	0.64	0.10	0.73

A similar process is applied to the phase difference scores. Considering the example, the relative power score in the subacute phase is 0.64. The phase difference score therefore is -0.07 (subacute score minus acute score, see bottom row in Table 19Tabel 20). In this patient, the difference in phases with the highest score is 0.13 at C3 and the lowest is -0.07 at O2 (see Tabel 20).

The process as described above is applied similarly to all other patients. This way a dataset is created for highest and lowest values for the acute phase, subacute phase and phase difference, for all frequency bands and for both eye states. These sets were statistically compared to the HISC scores and the GOS-E outcomes. Figure 16 and Figure 17 are examples of visualisations of these comparisons. These plots visualise the alpha band, eyes closed setting, which is the same setting as in the example.

The dataset shown in Figure 16 has, in comparison to the HISC scores, a correlation value of 0.17 and a significance value of 0.43. In this case, the correlation value is fairly low, indicating a poor correlation. The correlation is visualised by the trendline in the scatterplot. The almost horizontal trendline (compared to the vertical range of the datapoints) coincides with a poor correlation. It seems that all patients had higher relative alpha power scores than the healthy average (zero value line).

Figure 17 shows the difference between the good GOS-E outcome and poor outcome group. This comparison scores a significance value of 0.15. Compared to the good GOS-E group, patients with a poor GOS-E outcome tend to have higher relative alpha power scores in the acute phase, considering the aforementioned setting. Both groups score above healthy average (zero value line).

Tabel 20. Example of the divergence-selection-algorithm processing of phase difference data. This table represents data from one patient. The phase difference scores (fourth column) are calculated by subtracting the acute phase scores (third column) from the subtracting the acute phase scores (third column) from the subacute phase scores (second column). Per patient, the highest and lowest scoring leads are selected (green and red respectively).

Lead	Scores subacute phase	Scores acute phase	Phase difference scores
Fp1	0.52	0.44	0.09
Fp2	0.50	0.43	0.07
F7	0.49	0.42	0.07
F3	0.55	0.45	0.09
Fz	0.56	0.47	0.09
F4	0.53	0.49	0.04
F8	0.47	0.41	0.07
T3	0.43	0.37	0.06
C3	0.50	0.37	0.13
Cz	0.54	0.49	0.05
C4	0.49	0.44	0.05
T4	0.40	0.33	0.07
T5	0.52	0.53	-0.01
P3	0.46	0.44	0.03
Pz	0.45	0.41	0.05
P4	0.54	0.48	0.06
T6	0.67	0.55	0.12
O1	0.67	0.70	-0.03
O2	0.64	0.71	-0.07

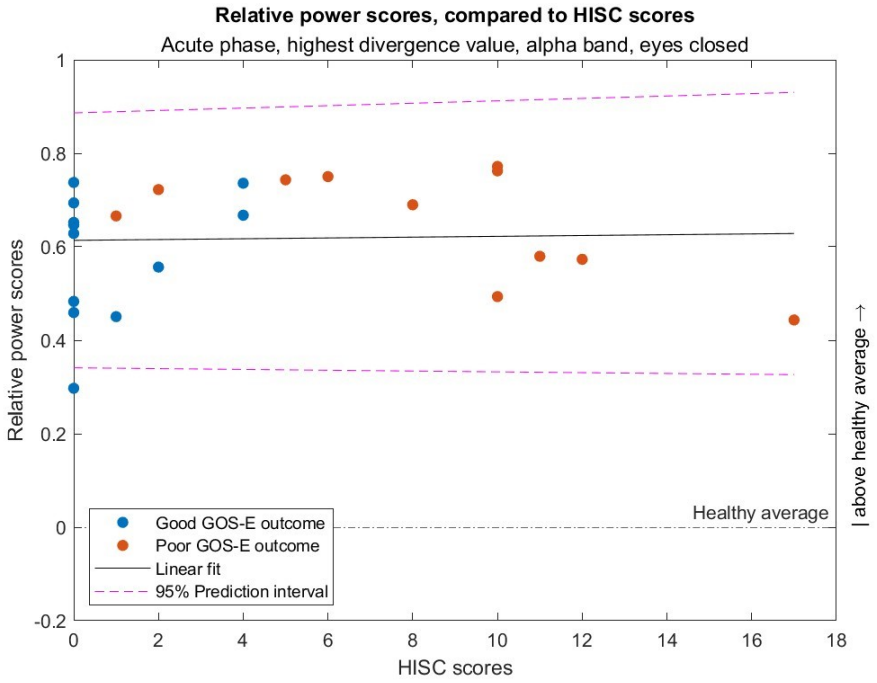

Figure 16. Example of a visualisation of the HISC-score – relative power scores comparison. In this case, no strong correlation can be seen; the trendline is close to horizontal, compared to the vertical range of the datapoints. This coincides with the correlation value of 0.17, found when applying the Spearmans Correlation coeficient test.

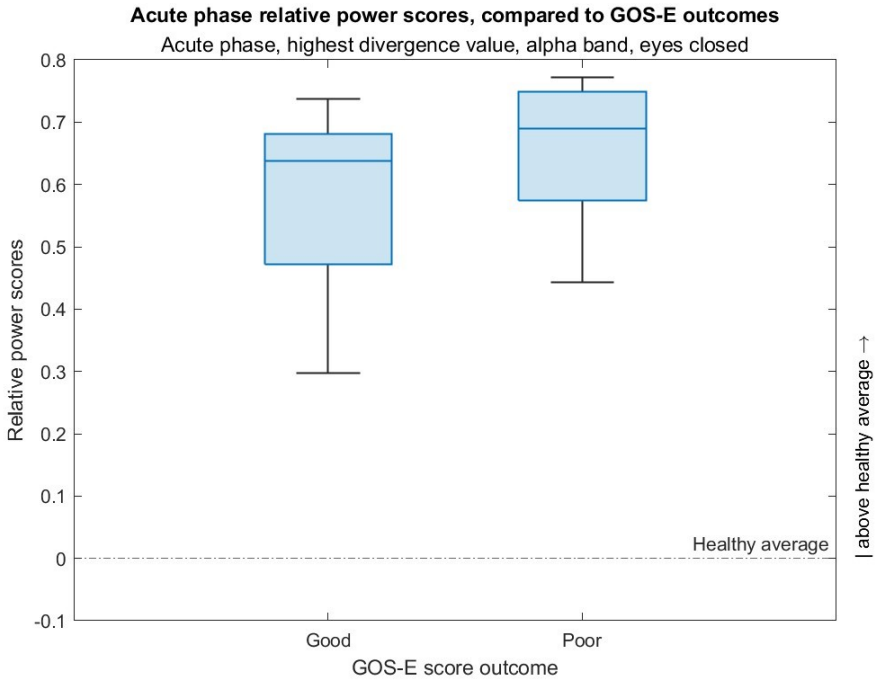

Figure 17. Example of a visualisation of the GOS-E outcome – relative power scores comparison. In this case, the Mann-Whitney U test did not prove a significant result (P = 0.15). It seems that all patients score higher relative alpha powers than healthy average. The poor outcome group seems to score on average higher than the good outcome group.

Appendix 5 – All HISC and GOS-E comparison results

Table 21. Overview of all HISC comparison results, ordered by statistical relevance (based on absolute correlation scores). Cor. – Correlation score, abs Cor. – Absolute correlation score, P – Statistical significance value.

Approach	Phase	Band	Divergence	Eye state	Cor.	abs Cor.	P
Relative power	Difference	Alpha	Highest	Closed	-0.43	0.43	0.04
Power variability	Subacute	Theta	Highest		-0.43	0.43	0.03
Power symmetry	Difference		Highest	Open	-0.37	0.37	0.08
Power symmetry	Acute		Highest	Closed	0.36	0.36	0.09
Power symmetry	Subacute		Lowest	Open	-0.34	0.34	0.09
Relative power	Difference	Theta	Lowest	Closed	0.33	0.33	0.12
Coherence	Acute		Lowest	Open	-0.33	0.33	0.12
Relative power	Subacute	Alpha	Lowest	Open	0.30	0.30	0.14
Power variability	Subacute	Beta	Lowest		0.29	0.29	0.15
Power symmetry	Acute		Lowest	Closed	0.28	0.28	0.20
Power variability	Subacute	Alpha	Highest		-0.26	0.26	0.19
Relative power	Subacute	Alpha	Highest	Open	0.26	0.26	0.19
Coherence	Difference		Lowest	Open	0.26	0.26	0.23
Coherence	Acute		Lowest	Closed	-0.26	0.26	0.23
Coherence	Difference		Lowest	Closed	0.24	0.24	0.27
Power symmetry	Subacute		Highest	Open	-0.24	0.24	0.24
Relative power	Difference	Alpha	Highest	Open	0.24	0.24	0.28
Coherence	Subacute		Lowest	Open	0.22	0.22	0.29
Power variability	Acute	Theta	Highest		-0.21	0.21	0.34
Power variability	Subacute	Theta	Lowest		0.21	0.21	0.31
Power variability	Difference	Alpha	Highest		-0.20	0.20	0.35
Power variability	Difference	Beta	Highest		-0.20	0.20	0.35
Power variability	Difference	Theta	Highest		-0.20	0.20	0.35
Power variability	Subacute	Alpha	Lowest		0.20	0.20	0.33
Coherence	Difference		Highest	Closed	0.19	0.19	0.38
Coherence	Subacute		Lowest	Closed	0.18	0.18	0.37
Coherence	Acute		Highest	Closed	0.18	0.18	0.42
Coherence	Difference		Highest	Open	0.18	0.18	0.42
Relative power	Subacute	Beta	Lowest	Open	0.18	0.18	0.39
Relative power	Difference	Theta	Lowest	Open	-0.17	0.17	0.43
Relative power	Acute	Alpha	Highest	Closed	0.17	0.17	0.43
Relative power	Subacute	Beta	Highest	Open	-0.17	0.17	0.40
Relative power	Difference	Alpha	Lowest	Open	0.17	0.17	0.44
Relative power	Acute	Alpha	Lowest	Closed	0.15	0.15	0.51
Relative power	Acute	Alpha	Highest	Open	0.14	0.14	0.52
Relative power	Difference	Theta	Highest	Closed	0.14	0.14	0.53
Relative power	Subacute	Theta	Highest	Open	-0.13	0.13	0.53
Power symmetry	Difference		Lowest	Closed	-0.13	0.13	0.57

Relative power	Difference	Alpha	Lowest	Closed	-0.12	0.12	0.58
Coherence	Subacute		Highest	Closed	0.12	0.12	0.56
Coherence	Subacute		Highest	Open	0.11	0.11	0.59
Power symmetry	Difference		Highest	Closed	-0.11	0.11	0.62
Relative power	Subacute	Theta	Highest	Closed	0.10	0.10	0.62
Relative power	Subacute	Theta	Lowest	Closed	0.10	0.10	0.64
Power variability	Acute	Theta	Lowest		0.10	0.10	0.66
Relative power	Acute	Theta	Lowest	Closed	-0.10	0.10	0.67
Power symmetry	Acute		Lowest	Open	0.09	0.09	0.68
Relative power	Acute	Beta	Highest	Closed	-0.08	0.08	0.72
Relative power	Acute	Theta	Highest	Open	-0.07	0.07	0.74
Relative power	Acute	Theta	Highest	Closed	-0.07	0.07	0.76
Coherence	Acute		Highest	Open	0.07	0.07	0.76
Relative power	Acute	Alpha	Lowest	Open	0.06	0.06	0.77
Relative power	Difference	Beta	Highest	Open	0.06	0.06	0.77
Relative power	Acute	Beta	Highest	Open	-0.06	0.06	0.78
Relative power	Acute	Beta	Lowest	Open	0.06	0.06	0.78
Relative power	Difference	Beta	Highest	Closed	-0.06	0.06	0.79
Relative power	Subacute	Theta	Lowest	Open	0.05	0.05	0.82
Relative power	Difference	Beta	Lowest	Closed	0.05	0.05	0.83
Power variability	Subacute	Beta	Highest		0.05	0.05	0.83
Relative power	Subacute	Alpha	Lowest	Closed	-0.04	0.04	0.84
Relative power	Difference	Beta	Lowest	Open	-0.04	0.04	0.87
Relative power	Subacute	Beta	Highest	Closed	0.03	0.03	0.87
Relative power	Acute	Beta	Lowest	Closed	-0.03	0.03	0.88
Relative power	Difference	Theta	Highest	Open	-0.03	0.03	0.91
Power variability	Acute	Beta	Highest		-0.02	0.02	0.91
Power variability	Acute	Alpha	Highest		0.02	0.02	0.93
Power symmetry	Acute		Highest	Open	-0.02	0.02	0.94
Power symmetry	Subacute		Highest	Closed	0.02	0.02	0.93
Power symmetry	Subacute		Lowest	Closed	-0.01	0.01	0.94
Relative power	Subacute	Alpha	Highest	Closed	0.01	0.01	0.94
Relative power	Subacute	Beta	Lowest	Closed	-0.01	0.01	0.95
Power variability	Acute	Alpha	Lowest		-0.01	0.01	0.95
Power variability	Acute	Beta	Lowest		-0.01	0.01	0.97
Power symmetry	Difference		Lowest	Open	0.01	0.01	0.97
Relative power	Acute	Theta	Lowest	Open	0.00	0.00	0.98
Power variability	Difference	Alpha	Lowest		0.00	0.00	0.99
Power variability	Difference	Beta	Lowest		0.00	0.00	0.99
Power variability	Difference	Theta	Lowest		0.00	0.00	0.99

Table 22. Overview of all GOS-E comparison results, ordered by statistical relevance (based on significance values). P – Statistical significance value.

Approach	Phase	Band	Divergence	Eye state	Ranksum	P
Coherence	Acute		Lowest	Open	98	0.04
Relative power	Difference	Alpha	Highest	Closed	103	0.08
Coherence	Acute		Lowest	Closed	103	0.08
Power symmetry	Subacute		Lowest	Open	142	0.09
Relative power	Difference	Theta	Lowest	Closed	158	0.12
Relative power	Acute	Alpha	Highest	Closed	156	0.15
Power symmetry	Acute		Highest	Closed	156	0.15
Relative power	Acute	Theta	Lowest	Closed	110	0.19
Coherence	Difference		Lowest	Closed	154	0.19
Relative power	Subacute	Alpha	Highest	Open	201	0.20
Power symmetry	Subacute		Highest	Open	150	0.20
Power variability	Subacute	Beta	Lowest		200	0.20
Relative power	Difference	Theta	Highest	Closed	153	0.21
Coherence	Difference		Lowest	Open	153	0.21
Relative power	Subacute	Beta	Highest	Open	151	0.22
Relative power	Acute	Alpha	Lowest	Open	152	0.24
Power variability	Subacute	Beta	Highest		198	0.26
Power variability	Subacute	Alpha	Lowest		197	0.27
Relative power	Difference	Alpha	Lowest	Closed	114	0.29
Relative power	Acute	Alpha	Highest	Open	149	0.32
Power variability	Acute	Theta	Highest		116	0.35
Power symmetry	Acute		Lowest	Open	148	0.35
Power symmetry	Difference		Highest	Closed	116	0.35
Power symmetry	Difference		Highest	Open	116	0.35
Power variability	Acute	Theta	Lowest		147	0.38
Power symmetry	Difference		Lowest	Closed	117	0.38
Relative power	Subacute	Alpha	Lowest	Open	193	0.39
Power symmetry	Difference		Lowest	Open	146	0.41
Relative power	Subacute	Alpha	Highest	Closed	192	0.42
Relative power	Acute	Alpha	Lowest	Closed	145	0.45
Relative power	Acute	Beta	Highest	Open	119	0.45
Power variability	Subacute	Theta	Lowest		190	0.46
Relative power	Acute	Theta	Highest	Closed	120	0.49
Power variability	Acute	Alpha	Highest		143	0.53
Coherence	Acute		Highest	Open	121	0.53
Relative power	Subacute	Beta	Lowest	Closed	163	0.54
Coherence	Subacute		Lowest	Open	188	0.54
Relative power	Acute	Beta	Highest	Closed	122	0.57
Coherence	Difference		Highest	Closed	142	0.57
Power variability	Subacute	Theta	Highest		164	0.58
Relative power	Difference	Theta	Lowest	Open	124	0.65
Power variability	Acute	Alpha	Lowest		140	0.65

Power symmetry	Subacute		Highest	Closed	167	0.69
Power symmetry	Subacute		Lowest	Closed	184	0.69
Relative power	Acute	Theta	Highest	Open	125	0.69
Relative power	Difference	Alpha	Highest	Open	125	0.69
Relative power	Subacute	Theta	Lowest	Closed	168	0.72
Coherence	Subacute		Highest	Closed	168	0.72
Coherence	Subacute		Lowest	Closed	183	0.72
Relative power	Acute	Beta	Lowest	Closed	126	0.74
Relative power	Acute	Beta	Lowest	Open	126	0.74
Relative power	Difference	Theta	Highest	Open	138	0.74
Power symmetry	Acute		Highest	Open	126	0.74
Power symmetry	Acute		Lowest	Closed	138	0.74
Coherence	Acute		Highest	Closed	138	0.74
Relative power	Subacute	Theta	Lowest	Open	182	0.76
Coherence	Subacute		Highest	Open	169	0.76
Relative power	Acute	Theta	Lowest	Open	127	0.79
Relative power	Difference	Beta	Highest	Closed	127	0.79
Relative power	Subacute	Beta	Highest	Closed	170	0.80
Relative power	Subacute	Beta	Lowest	Open	171	0.84
Power variability	Subacute	Alpha	Highest		171	0.84
Relative power	Subacute	Alpha	Lowest	Closed	172	0.88
Power variability	Difference	Alpha	Lowest		129	0.88
Power variability	Difference	Beta	Lowest		129	0.88
Power variability	Difference	Theta	Lowest		129	0.88
Relative power	Difference	Alpha	Lowest	Open	134	0.93
Relative power	Difference	Beta	Lowest	Open	134	0.93
Power variability	Difference	Alpha	Highest		130	0.93
Power variability	Difference	Beta	Highest		130	0.93
Power variability	Difference	Theta	Highest		130	0.93
Coherence	Difference		Highest	Open	134	0.93
Power variability	Acute	Beta	Lowest		134	0.94
Relative power	Subacute	Theta	Highest	Closed	174	0.96
Relative power	Difference	Beta	Lowest	Closed	131	0.98
Power variability	Acute	Beta	Highest		131	0.98
Relative power	Difference	Beta	Highest	Open	132	1.00
Relative power	Subacute	Theta	Highest	Open	175	1.00

Table 23. Overview of all relative power HISC comparison results, ordered by phase. Cor. – Correlation score, abs Cor. – Absolute correlation score, P – Statistical significance value.

Phase	Band	Divergence	Eye state	Cor.	abs Cor.	P
Acute	Alpha	Lowest	Closed	0.15	0.15	0.51
Acute	Alpha	Lowest	Open	0.06	0.06	0.77
Acute	Alpha	Highest	Closed	0.17	0.17	0.43
Acute	Alpha	Highest	Open	0.14	0.14	0.52
Acute	Beta	Lowest	Closed	-0.03	0.03	0.88
Acute	Beta	Lowest	Open	0.06	0.06	0.78
Acute	Beta	Highest	Closed	-0.08	0.08	0.72
Acute	Beta	Highest	Open	-0.06	0.06	0.78
Acute	Theta	Lowest	Closed	-0.10	0.10	0.67
Acute	Theta	Lowest	Open	0.00	0.00	0.98
Acute	Theta	Highest	Closed	-0.07	0.07	0.76
Acute	Theta	Highest	Open	-0.07	0.07	0.74
Subacute	Alpha	Lowest	Closed	-0.04	0.04	0.84
Subacute	Alpha	Lowest	Open	0.30	0.30	0.14
Subacute	Alpha	Highest	Closed	0.01	0.01	0.94
Subacute	Alpha	Highest	Open	0.26	0.26	0.19
Subacute	Beta	Lowest	Closed	-0.01	0.01	0.95
Subacute	Beta	Lowest	Open	0.18	0.18	0.39
Subacute	Beta	Highest	Closed	0.03	0.03	0.87
Subacute	Beta	Highest	Open	-0.17	0.17	0.40
Subacute	Theta	Lowest	Closed	0.10	0.10	0.64
Subacute	Theta	Lowest	Open	0.05	0.05	0.82
Subacute	Theta	Highest	Closed	0.10	0.10	0.62
Subacute	Theta	Highest	Open	-0.13	0.13	0.53
Difference	Alpha	Lowest	Closed	-0.12	0.12	0.58
Difference	Alpha	Lowest	Open	0.17	0.17	0.44
Difference	Alpha	Highest	Closed	-0.43	0.43	0.04
Difference	Alpha	Highest	Open	0.24	0.24	0.28
Difference	Beta	Lowest	Closed	0.05	0.05	0.83
Difference	Beta	Lowest	Open	-0.04	0.04	0.87
Difference	Beta	Highest	Closed	-0.06	0.06	0.79
Difference	Beta	Highest	Open	0.06	0.06	0.77
Difference	Theta	Lowest	Closed	0.33	0.33	0.12
Difference	Theta	Lowest	Open	-0.17	0.17	0.43
Difference	Theta	Highest	Closed	0.14	0.14	0.53
Difference	Theta	Highest	Open	-0.03	0.03	0.91

Table 24. Overview of all relative power GOS-E comparison results, ordered by phase. P – Statistical significance value.

Phase	Band	Divergence	Eye state	Ranksum	P
Acute	Alpha	Lowest	Closed	145	0.45
Acute	Alpha	Lowest	Open	152	0.24
Acute	Alpha	Highest	Closed	156	0.15
Acute	Alpha	Highest	Open	149	0.32
Acute	Beta	Lowest	Closed	126	0.74
Acute	Beta	Lowest	Open	126	0.74
Acute	Beta	Highest	Closed	122	0.57
Acute	Beta	Highest	Open	119	0.45
Acute	Theta	Lowest	Closed	110	0.19
Acute	Theta	Lowest	Open	127	0.79
Acute	Theta	Highest	Closed	120	0.49
Acute	Theta	Highest	Open	125	0.69
Subacute	Alpha	Lowest	Closed	172	0.88
Subacute	Alpha	Lowest	Open	193	0.39
Subacute	Alpha	Highest	Closed	192	0.42
Subacute	Alpha	Highest	Open	201	0.20
Subacute	Beta	Lowest	Closed	163	0.54
Subacute	Beta	Lowest	Open	171	0.84
Subacute	Beta	Highest	Closed	170	0.80
Subacute	Beta	Highest	Open	151	0.22
Subacute	Theta	Lowest	Closed	168	0.72
Subacute	Theta	Lowest	Open	182	0.76
Subacute	Theta	Highest	Closed	174	0.96
Subacute	Theta	Highest	Open	175	1.00
Difference	Alpha	Lowest	Closed	114	0.29
Difference	Alpha	Lowest	Open	134	0.93
Difference	Alpha	Highest	Closed	103	0.08
Difference	Alpha	Highest	Open	125	0.69
Difference	Beta	Lowest	Closed	131	0.98
Difference	Beta	Lowest	Open	134	0.93
Difference	Beta	Highest	Closed	127	0.79
Difference	Beta	Highest	Open	132	1.00
Difference	Theta	Lowest	Closed	158	0.12
Difference	Theta	Lowest	Open	124	0.65
Difference	Theta	Highest	Closed	153	0.21
Difference	Theta	Highest	Open	138	0.74

Table 25. Overview of all power variability HISC comparison results, ordered by phase. Cor. – Correlation score, abs Cor. – Absolute correlation score, P – Statistical significance value.

Phase	Band	Divergence	Cor.	abs Cor.	P
Acute	Alpha	Lowest	-0.01	0.01	0.95
Acute	Alpha	Highest	0.02	0.02	0.93
Acute	Beta	Lowest	-0.01	0.01	0.97
Acute	Beta	Highest	-0.02	0.02	0.91
Acute	Theta	Lowest	0.10	0.10	0.66
Acute	Theta	Highest	-0.21	0.21	0.34
Subacute	Alpha	Lowest	0.20	0.20	0.33
Subacute	Alpha	Highest	-0.26	0.26	0.19
Subacute	Beta	Lowest	0.29	0.29	0.15
Subacute	Beta	Highest	0.05	0.05	0.83
Subacute	Theta	Lowest	0.21	0.21	0.31
Subacute	Theta	Highest	-0.43	0.43	0.03
Difference	Alpha	Lowest	0.00	0.00	0.99
Difference	Alpha	Highest	-0.20	0.20	0.35
Difference	Beta	Lowest	0.00	0.00	0.99
Difference	Beta	Highest	-0.20	0.20	0.35
Difference	Theta	Lowest	0.00	0.00	0.99
Difference	Theta	Highest	-0.20	0.20	0.35

Table 26. Overview of all power variability GOS-E comparison results, ordered by phase. P – Statistical significance value.

Phase	Band	Divergence	Ranksum	P
Acute	Alpha	Lowest	139.5	0.65
Acute	Alpha	Highest	143	0.53
Acute	Beta	Lowest	133.5	0.94
Acute	Beta	Highest	131	0.98
Acute	Theta	Lowest	146.5	0.38
Acute	Theta	Highest	116	0.35
Subacute	Alpha	Lowest	197	0.27
Subacute	Alpha	Highest	171	0.84
Subacute	Beta	Lowest	200	0.20
Subacute	Beta	Highest	198	0.26
Subacute	Theta	Lowest	190	0.46
Subacute	Theta	Highest	164	0.58
Difference	Alpha	Lowest	129	0.88
Difference	Alpha	Highest	130	0.93
Difference	Beta	Lowest	129	0.88
Difference	Beta	Highest	130	0.93
Difference	Theta	Lowest	129	0.88
Difference	Theta	Highest	130	0.93

Table 27. Overview of all power symmetry HISC comparison results, ordered by phase. Cor. – Correlation score, abs Cor. – Absolute correlation score, P – Statistical significance value.

Phase	Divergence	Eye state	Cor.	abs Cor.	P
Acute	Lowest	Closed	0.28	0.28	0.20
Acute	Lowest	Open	0.09	0.09	0.68
Acute	Highest	Closed	0.36	0.36	0.09
Acute	Highest	Open	-0.02	0.02	0.94
Subacute	Lowest	Closed	-0.01	0.01	0.94
Subacute	Lowest	Open	-0.34	0.34	0.09
Subacute	Highest	Closed	0.02	0.02	0.93
Subacute	Highest	Open	-0.24	0.24	0.24
Difference	Lowest	Closed	-0.13	0.13	0.57
Difference	Lowest	Open	0.01	0.01	0.97
Difference	Highest	Closed	-0.11	0.11	0.62
Difference	Highest	Open	-0.37	0.37	0.08

Table 28. Overview of all power symmetry GOS-E comparison results, ordered by phase. P – Statistical significance value.

Phase	Divergence	Eye state	Ranksum	P
Acute	Lowest	Closed	138	0.74
Acute	Lowest	Open	148	0.35
Acute	Highest	Closed	156	0.15
Acute	Highest	Open	126	0.74
Subacute	Lowest	Closed	184	0.69
Subacute	Lowest	Open	142	0.09
Subacute	Highest	Closed	167	0.69
Subacute	Highest	Open	150	0.20
Difference	Lowest	Closed	117	0.38
Difference	Lowest	Open	146	0.41
Difference	Highest	Closed	116	0.35
Difference	Highest	Open	116	0.35

Table 29. Overview of all Coherence HISC comparison results, ordered by phase. Cor. – Correlation score, abs Cor. – Absolute correlation score, P – Statistical significance value.

Phase	Divergence	Eye state	Cor.	abs Cor.	P
Acute	Lowest	Closed	-0.26	0.26	0.24
Acute	Lowest	Open	-0.33	0.33	0.12
Acute	Highest	Closed	0.18	0.18	0.42
Acute	Highest	Open	0.07	0.07	0.76
Subacute	Lowest	Closed	0.18	0.18	0.37
Subacute	Lowest	Open	0.22	0.22	0.29
Subacute	Highest	Closed	0.12	0.12	0.56
Subacute	Highest	Open	0.11	0.11	0.59
Difference	Lowest	Closed	0.24	0.24	0.27
Difference	Lowest	Open	0.26	0.26	0.23
Difference	Highest	Closed	0.19	0.19	0.38
Difference	Highest	Open	0.18	0.18	0.42

Table 30. Overview of all Coherence GOS-E comparison results, ordered by phase. P – Statistical significance value.

Phase	Divergence	Eye state	Ranksum	P
Acute	Lowest	Closed	103	0.08
Acute	Lowest	Open	98	0.04
Acute	Highest	Closed	138	0.74
Acute	Highest	Open	121	0.53
Subacute	Lowest	Closed	183	0.72
Subacute	Lowest	Open	188	0.55
Subacute	Highest	Closed	168	0.72
Subacute	Highest	Open	169	0.76
Difference	Lowest	Closed	154	0.19
Difference	Lowest	Open	153	0.21
Difference	Highest	Closed	142	0.57
Difference	Highest	Open	134	0.93